A SMART RESTORATION TECHNIQUE FOR MULTI-MICROGRID DISTRIBUTION SYSTEMS

BY

MOHEEB KAMAL OTT

A Thesis Presented to the

DEANSHIP OF GRADUATE STUDIES

KING FAHD UNIVERSITY OF PETROLEUM & MINERALS

DHAHRAN, SAUDI ARABIA

In Partial Fulfillment of the
Requirements for the Degree of

MASTER OF SCIENCE

In

ELECTRICAL ENGINEERING

March 2018

KING FAHD UNIVERSITY OF PETROLEUM & MINERALS

DHAHRAN- 31261, SAUDI ARABIA

DEANSHIP OF GRADUATE STUDIES

This thesis, written by **MOHEEB KAMAL OTT** under the direction his thesis advisor

and approved by his thesis committee, has been presented and accepted by the Dean of

Graduate Studies, in partial fulfillment of the requirements for the degree of   **MASTER**

OF SCIENCE IN ELECTRICAL ENGINEERING.

Dr. Mohammed Al-Muhaini
(Advisor)

Dr. Ali Al-Shaikhi
Department Chairman

Dr. Mohammed Abido
(Member)

Dr. Salam Zummo
Dean of Graduate Studies

Dr. Mahmoud Kassas
(Member)

28/3/12

Date

To my parents, brothers and sisters and friends.

ACKNOWLEDGMENTS

My great thanks and appreciation to King Fahd University of Petroleum & Minerals and the Electrical Engineering Department for providing support and great educational platform during my study.

I would like to express my sincere gratitude to my advisor, Dr. Mohammed AlMuhaini, for his guidance, patience, motivation and continuous support during the course of my research. His guidance, support and constructive insights were crucial for the successful completion of this thesis. It was a great honor to work under his supervision.

Besides my advisor, I would also like to thank the rest of my thesis committee members, Dr. Mohammed Abido and Dr. Mahmoud Kassas, for their time, insightful comments and feedbacks. Their academic support and critical reviews are deeply appreciated.

Last but not least, I would like to express my deep gratitude to my family and close friends for their unfailing love and unconditional support during all the stages of my study. They were always there for me through nice and tough times. Words are not sufficient to express how grateful I am for having them in my life.

TABLE OF CONTENTS

LIST OF TABLES

LIST OF FIGURES

LIST OF ABBREVIATIONS

AMI   :   Advanced Metering Infrastructure

BESS   :   Battery Energy Storage System

DG   :   Distributed Generators

DR   :   Demand Response

DSM   :   Demand Side Management

EMS   :   Energy Management System

ESS   :   Energy Storage System

EV   :   Electric Vehicle

FESS   :   Flywheel Energy Storage Systems

LP   :   Linear Programming

MILP   :   Mixed Integer Linear Programming

MMG   :   Multi-Microgrids

PPC   :   Point of Common Coupling

PV   :   Photovoltaic

RH   :   Rolling Horizon

SEMS   :   Superconducting Magnetic Energy Storage

SI	:	Success Index
STC	:	Standard Test Conditions
UCES	:	Ultra-Capacitor Energy Storage

NOMENCLATURE

Indices:

t	Index of time slot
i	Index of microgrid
g	Index of conventional DG unit
r	Index of renewable DG unit
l	Index of load point
s	Index of ESS unit
n	Index of allowable surplus power utilization interval of conventional DG

Parameters and constants:

N_g	Number of conventional DG units
N_r	Number of renewable DG units
N_s	Number of ESS units
N_l	Number of load points
T_{local}	Horizon of local scheduling optimization
T_{shift}	Horizon of preemptive load shifting signal generation
T_{emrg}	Expected duration of emergency
Δt	Time slot duration
C^{CG}	Cost of conventional DG unit generation
C^{RG}	Cost of renewable DG unit generation
C^{Shed}	Cost of load shedding
C^{Ch}	Cost of charging of ESS

C^{Dch}	Cost of discharging of ESS
DR	Maximum ramp down rate of conventional DG
UR	Maximum ramp up rate of conventional DG
UT	Minimum up time of conventional DG
DT	Minimum down time of conventional DG
T^{on}	Duration in which conventional DG was ON
T^{off}	Duration in which conventional DG was OFF
X	Conventional DG unit availability indicator
P^{Load}	Demand of load point
η^{ch}	Charging efficiency of ESS
η^{dch}	Discharging efficiency of EES
τ_{IJ}	Availability of tie line between microgrid i and microgrid j
$T^{max}{}_{ij}$	Maximum capacity of tie line between microgrid i and microgrid j
e	Emergency starting time

Variables:

P^{CG}	Conventional DG generation
I	Conventional DG commitment indicator
X	Conventional DG availability indicator
u	Conventional DG startup indicator
d	Conventional DG shutdown indicator
P^{RG}	Renewable DG generation
P^{Shed}	Amount of load shedding (local scheduling)
P^{Ch}	Power charging rate of ESS

P^{Dch}	Power discharging rate of ESS
ch	ESS charging indicator
dch	ESS unit discharging indicator
CG	Utilized surplus power from conventional DG
Z	Interval indicator of utilized surplus power from conventional DGs
RG	Utilized surplus power from renewable DG
ES	Utilized surplus power from ESS
$T_{ij,t}^{+}$	Power transferred to microgrid i from microgrid j
$T_{ij,t}^{-}$	Power transferred to microgrid i from microgrid j
LS	Amount of load shedding (global scheduling)

Symbols and abbreviations:

$-adj$	Adjustable power (surplus power)
I	Optimal value after local scheduling
II	Optimal value after global scheduling
max	Maximum
min	Minimum
LP	Low Priority
MP	Medium Priority
HP	High Priority

ABSTRACT

Full Name   : [Moheeb Kamal Ott]

Thesis Title   : [A Smart Restoration Technique for Multi-Microgrid Distribution Systems]

Major Field   : [Electrical Engineering

Date of Degree : [March 2018]

Modern and industrial societies require a high-quality, secure and reliable power supply that meets their energy demand. As this demand is increasing with time, while the network infrastructure is aging, the reliability, quality and resilience of the power grid are becoming major concerns. This argument is proven to be true by the occurrence of several major blackouts in the existing power systems over the course of the last decades. To resolve the root causes of the shortages in the current power systems, the concepts of smart and microgrids were developed. One of the main characteristics of the future smart grids is their ability to withstand low-frequent high-impact disturbances and to recover outages quickly and efficiently. In this context designing and developing of an efficient and rapid load restoration techniques is an essential component of realizing the future smart grids.

The focus of this thesis is the outage management of interconnected microgrids during islanded operation after being disconnected from the utility main supply. A proposed two-stage load restoration technique is formed as a Mixed Integer Linear Programming (MILP) optimization problem whose objective is optimally restoring the maximum number of disconnected loads. The proposed technique is applied to a distribution system composed of several microgrids, i.e. Multi-Microgrid (MMG) distribution system. In this proposed technique, the power transactions between the individual microgrid are managed after the schedule of local energy resources and the control signals of local flexible loads are determined. Flexible loads control signals are decided through two incorporated Demand Side Management (DMS) programs namely, emergency load shedding and preemptive Load shifting.

Each microgrid is assumed to be composed of local conventional and renewable Distributed Generators (DGs) and Energy Storage System (ESS) in addition to a flexible load. In order to quantify the performance of the restoration technique, a new index, restoration technique success index (SI) was also proposed. The effectiveness of the proposed restoration technique is testified through comprehensive test case scenarios and numerical simulations. In addition, the impact of different parameters on the performance of the restoration technique is analyzed by conducting sensitivity analysis.

ملخص الرسالة

الاسم الكامل: مهيب كمال العط

عنوان الرسالة: أسلوب ذكي لاستعادة الأحمال الكهربائية المفصولة لشبكات التوزيع الكهربائي المكونة من عدد من الشبكات المتناهية الصغر (Microgrids).

التخصص: الهندسة الكهربائية

تاريخ الدرجة العلمية: رجب 1439

تتطلب المجتمعات الحديثة والصناعية إمدادات طاقة كهربائية عالية الجودة، وآمنة، يمكن الاعتماد عليها لتلبي احتياجاتها من الطاقة. رجوعاً إلى حقيقة أن استهلاك الطاقة الكهربائية في ازدياد، في حين أن البنية التحتية للشبكة الكهربائية تزداد في العمر دون تغير، هذا أدى الى ازدياد المخاوف بشأن موثوقية و جودة الطاقة، و مرونة شبكة الكهرباء في مواجهة انقطاعات الخدمة الكهربائية التي تسببها الكوارث الطبيعية. بدا ضعف شبكات الطاقة الكهربائية الحالية جلياً حيث حدثت العديد من حالات انقطاع الكهرباء الكبيرة في العقود القليلة الماضية. جاء تطوير مبدأ الشبكات الكهربائية الذكية (Smart Grids) والشبكات الكهربائية المتناهية الصغر(Microgrids) كحل مرشح لعيوب شبكات النقل الكهربائية التقليدية. وتتمثل إحدى أهم خصائص هذه الشبكات بقدرتها على تحمل الاضطرابات عالية التأثير منخفضة التواتر وقدرتها على استعادة الأحمال الكهربائية المقطوعة بسرعة وكفاءة عالية. بناء على ما سبق، يجدر القول إن تصميم وتطوير أساليب استعادة الأحمال الكهربائية المقطوعة بكفاءة وسرعة يعد عنصرا أساسيا في تحقيق بناء الشبكات الذكية المستقبلية. العمل المنجز في هذه الأطروحة يتعلق في إدارة تشغيل الشبكات الكهربائية المكونة من عدد من الشبكات الكهربائية المتناهية الصغر(Microgrids)عند تعذر الوصول الى إمدادات الطاقة الكهربائية من شبكة الكهرباء الرئيسة عقب تعرض الشبكة لطارئ كبير. لقد تم تصميم اسلوب ذكي يتكون من عدة خطوات على هيئة مشكلة إيجاد الحل الأمثل (Optimization Problem) باستخدام البرمجة الخطية وبرمجة الأرقام الصحيحة (Mixed Integer Linear Programing) بهدف استعادة أكبر قدر من الأحمال المقطوعة بأقل تكلفة ممكنة، هذا الأسلوب صمم ليطبق على شبكات التوزيع الكهربائي المكونة من عدد من الشبكات الكهربائية المتناهية الصغر، حيث يتم جدولة مصادر الطاقة والأحمال الكهربائية داخل كل شبكة من هذه الشبكات ومن ثمة إدارة تبادل الطاقة بينها. أُفترض أن كل شبكة من هذه الشبكات الكهربائية المتناهية الصغر(Microgrids) تتكون من عدد

من مصادر الطاقة الموزعة التقليدية منها والمتجددة، ونظام لحفظ وتخزين الطاقة وعدد من الأحمال الكهربائية المرنة والقابلة للتحكم. لقد تم إجراء تحليل في حساسية أداء أسلوب الاستعادة لعدة عوامل، على سبيل المثال، في تأثير تضمين برامج استجابة جانب الطلب على أداء أسلوب الاستعادة. لقد تم أيضا اقتراح مؤشر مبتكر لتكميم أداء اسلوب الاستعادة. عدة عمليات محاكاة عددية أجريت أخيرا للتدليل على كفاءة الأسلوب المقترح.

CHAPTER1

INTRODUCTION

Resiliency of smart distribution systems against contingencies and major events is expected to be one of the principal properties in the future according to the U.S. Department of Energy (DOE) [1]. As defined, resiliency is the ability of the system to withstand low-frequent, high-impact and wide-area disturbances and to recover interrupted consumers quickly and efficiently [2].

On the system level, the resiliency can be improved by hardening the infrastructure or improving the recovery and survival abilities of the power system [3]. Every change in the design, the construction guidelines, or the characteristics and features of the system building components is considered infrastructure hardening. Increasing the number of the underground cables, moving the feeders into safer paths and deploying better quality of transmission towers and poles are some examples of hardening the power system infrastructure, to name a few.

This thesis concerned in enhancing the outage recovery and survivability of the power system by proposing a smart load restoration technique. The restoration technique is designed and applied to Multi-Microgrid (MMG) distribution systems working on islanded operation after contingencies. Recovery and survivability can be defined in the context of this work as the ability of islanded microgrids to continue the same or near level of normal functioning without the gaining of the full power support from the main grid.

The function of the restoration technique is to define the system response to contingencies to maximize the number of recovered unserved loads at the least possible cost. The design of resiliency-based restoration technique is challenging considering the lack of precise prediction of contingencies incident and clearing times. Load restoration can be designed to be applied on several stages and includes many strategies and components where for example Demand Side Management (DSM) programs alongside with Energy Management System (EMS) can be applied. EMS is responsible for controlling the output of the resources in the system and maintain power balance. The is usually done by formulating an optimization problem with an objective of minimizing the operational cost of the system while meeting the load. The solution of the formulated problem is the schedule of the unit commitment and dispatch of the Distributed Generators (DGs) and charging and discharging of energy storage units within the system. The solution of the optimization problem must be feasible in which it does not violate the constraints of the system, such as the power balance of the system, the operational constraints of the DGs and charging and discharging limits of the energy storage units.

1.1   Motivation

With the growing development of modern industry and the increasing electrification of civilized societies, the reliance and the demand on electrical power is increasing [4]. As a result, the impact of any outage, especially catastrophic outages, is becoming more severe than before. Several sources showed that the number and cost of power outages are significantly high. For example, a report from North American Electric Reliability

Corporation (NERC), states that 80% of all outages in the US between 2003-2012 were weather-driven, causing around 147 million customers to lose their power supply for at least one hour [5]. Moreover, another statistic from US DOE stated that weather driven sustained service interruptions in the United States costs an average of US$18 to US$33 billion per year [6]. Considering the above-mentioned arguments and the fact that the frequency and strength of natural disasters is expected to increase [7] beside the rise in power consumption, enhancing the system resiliency and reliability is demanded more than ever.

Thus, it is valuable to develop efficient smart load restoration technique that minimizes outage durations and the number of the interrupted customers by optimally utilizing the resources and controllable loads. Additionally, the benefits of this technique are apparently extended to both customers and power utilities which makes more appreciable.

1.2 Objectives

The primary objective of this thesis is to propose a load restoration technique for distribution system composed of multiple microgrids being disconnected of the main utility grid after contingencies. The restoration scheme should be able to restore and supply as much as possible of the interrupted load for extended contingencies durations. The objectives of this thesis can be summarized in the following points:

i. To model the main components of microgrids including Energy Storage Systems (ESSs) and (DGs). The outputs of those models are used as an input to the restoration technique formulation.

ii. To propose a load restoration technique for Multi-Microgrids distribution systems.

iii. To study the impact of different parameters corresponding to renewable resources, energy storage units and demand response on the performance of the restoration technique.

iv. To analyze the performance of the restoration technique through various case studies.

1.3 Contributions

The main contribution of this thesis can be summarized as follows:

- A proposed novel two-stage restoration technique to supply and restore disconnected loads during and after outages was proposed. Furthermore, two Demand Response (DR) programs are defined and incorporated to the proposed restoration technique, namely preemptive load shifting and emergency load shedding programs. Preemptive load shifting is performed as the first step of the restoration plan in a practical way to enhance the restoration process. In this program, load shifting signals are generated and announced to customers in order to reshape their consumption pattern in accordance with the availability of resources. The proposed restoration technique stages are formulated as mixed

4

integer linear programming optimization problem which can be easily implemented and solved by available commercial solvers such as CPLEX [8].

- A new index, restoration technique success index (SI), is proposed to reflect the performance of the proposed technique. The index is calculated basically by comparing the ability of the system to restore disconnected loads in response to outages with and without applying the proposed technique measures.

1.4   Thesis Outline

In chapter 2, a literature survey is performed where the concept of smart grids and microgrids is introduced. In addition, past work done in literature about enhancing their resiliency and load restoration is presented. In chapter 3, a brief introduction about the building components of the system in addition to their adopted mathematical modelling is given. The problem formulation and the development of the proposed restoration technique in addition to the mathematical optimization technique used is discussed and explained in chapter 4. In chapter 5, test case scenarios are performed and discussed alongside different sensitivity analyses. Finally, in chapter 6, a conclusion, recommendations and future work that in row is stated.

CHAPTER 2

Literature Survey

2.1   Smart Grids

Conventionally, electrical energy is supplied to endpoint users in a radial one-way path. The power is typically generated from central large-scale electrical generation plants located far from the endpoint loads whether it was residential, commercial or industrial. The dominant portion of energy, served by conventional power systems, is produced from fossil-fueled power plants, mainly natural gas and coal plants, nuclear plants, and hydropower plants [9]. The generated power is stepped up to be transmitted through transmission system, mainly via overhead lines, over long distances. Finally, the power is stepped down to be supplied to endpoint consumers through the distribution system. The topolopy of a typical conventional power system is shown in Figure 2.1 that presumes a unidirectional energy delivery and information paths from the supplier to the customer. Such an architecture of power systems proved some deficiencies and resiliency issues especially against large catastrophes and disasters.

The concept of smart-grids is introduced to overcome these deficiencies and to improve the quality and the standards of energy generation, transmission and distribution. Smart-grids are regarded as the updated version of the current power systems where it facilitates the integration of the conventional power grid and new technologies to provide efficient energy supply and increase environmental benefits [10].
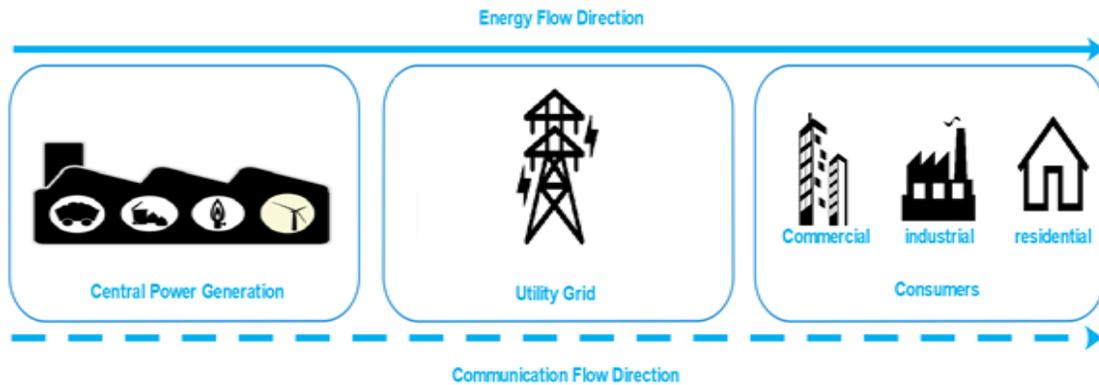
Figure 2.1 Conventional Power System Topology

The US Department of Energy (DOE) states that smart grids will have principal characteristics that include [11]:

1- Self-healing:

The grid will be able to detect, isolate and respond to the faults in a fast and an efficient manner in order to minimize the time and the area of any probable interruption.

2- Customer interactive:

The grid will be interactive with the customers and offer them several options to control their energy consumption by setting a real-time or semi-real-time electricity pricing, give them a choice to join several DMS programs, and facilitate their participation in energy generation.

3- High power quality:

The grid should maintain an appropriate power delivery which meets the needs of sensitive loads of the 21st-century such as robotics and electronic ships manufacturers. In other words, the power should be free of sags, spikes or any other power quality disturbances.

7

4- Optimized and efficient operation:

The grid will have smart algorithms and devices that will analyze and predict the status and the condition of the grid and generates suitable corrective or supportive actions to prevent outages and quality disturbances.

5- Integration of DG and distributed ESS:

The grid will be able to accommodate and control small-scale decentralized DGs, both conventional and renewable, beside different options of electrical storage devices.

In order to realize the concept of smart grids, many technologies have to be developed and deployed in their infrastructure [12]. For instance, one high-speed, reliable, and fully interconnected communication technologies that allow the components of the grid to communicate with each other by sending and receiving data and commands. The hardware components of the grid have to acquire the latest research development in materials, superconductivity, power electronics and microelectronics. Modern control methods and instrumentation have also to be deployed to the grid including advanced analytical and operational tools and algorithms and latest sensing and measuring technologies and applications such as advanced metering infrastructure (AMI). This will allow the grid to analyze and predict the condition of the grid and produce any necessary corrective actions. The structure of a smart grid is depicted in Figure 2.2, where components of the grid are interconnected and the energy storage and generation units are distributed unlike conventional power systems.
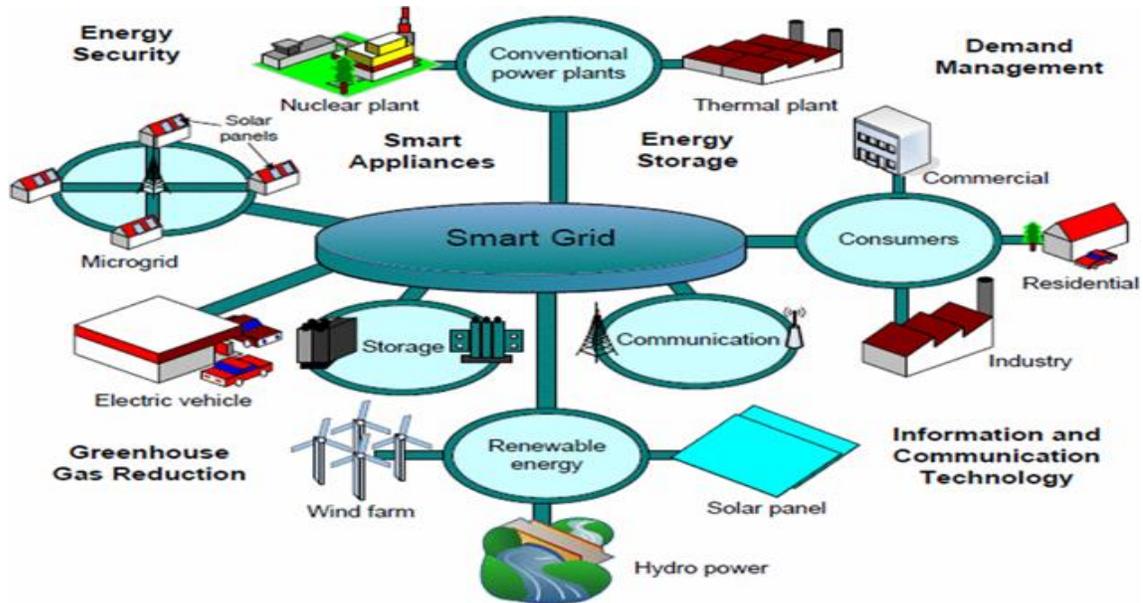
Figure 2.2 Smart Grid Overview [13]

2.2 Microgrids

Demand profile is increasing, and the peak demand is expected to increase by more than 50% from 2010 to 2040 [4]. The deployment of renewable DGs is considered as one of the key solutions to meet this expanding demand and reliance on renewables expected increase to the double by 2030 [14]. However, integrating renewable DGs to the grid can cause difficulties in maintaining the transient and steady stability of the power system as they are intermittent in nature and have very small inherited inertia as compared to bulk generation. The concept of microgrids was firstly introduced in technical literature as a solution to resolve those difficulties caused by the integration of distributed generation in a decentralized fashion to instead of dealing with complexity of addressing different difficulties facing the grid at the same time [15]. Thus, microgrid development can be regarded as the main building block in realizing future smart grids, and the main grid sees

9

it as a single component that responds to suitable control signals. Microgrids mainly consist of a cluster of DGs including both renewable and conventional fuel-based generators, a ESS mainly supercapacitors, batteries and flywheels, and finally a group of controllable and non-controllable loads. Microgrids can work in two modes of operation which are islanded mode and grid-connected mode [15] [17]. In grid-connected mode, the microgrid is connected to the main grid at the distribution level through the Point of Common Coupling (PCC). The deficit active and reactive power is supplied from the main grid, while the extra power can be sold to the main grid. In the islanded mode, microgrids are responsible for controlling the output of all micro resources, the charging and discharging rates of energy storage systems and generating appropriate signals to controllable loads in order to achieve a balance between demand and generation. Microgrids can be DC, AC or hybrid in which different suitable power electronics interfaces must exist in each of them. Figure 2.3 shows the typical block diagram of DC Microgrids, where distributed generators, storage devices, and loads are grouped to form what can be considered as a low-voltage sub-distribution system.
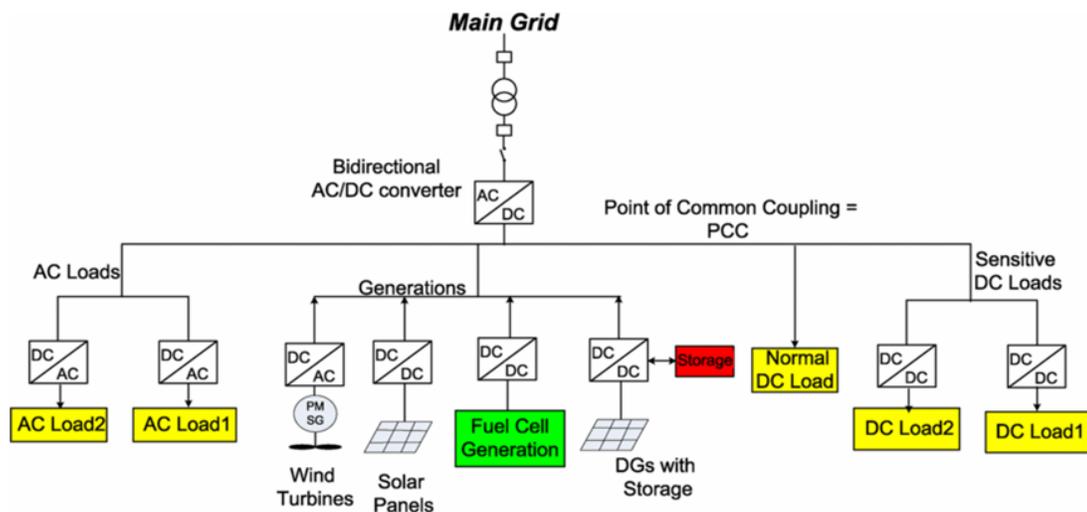
Figure 2.3 Structure of DC Microgrid [18]

2.2.1 Control of Microgrids

The control system of the microgrid must be able to achieve reliable and cost-efficient operation of microgrids in both modes of operations islanded and grid-connected modes. Furthermore, the microgrid control system has to ensure a smooth and seamless transition between modes of operations. The primarily controlled variables managed by microgrids control system are output active and reactive power of the distributed generators, and the voltage level and frequency of the micrgrid. Microgrids control systems can be categorized in respect of architecture into centralized and decentralized controls. In centralized microgrid control approach, the data is gathered and transmitted to one central controller that performs all the analysis and calculations and decides the actions needed to control all the components of the microgrid. On the other hand, in decentralized control approach, grid elements are controlled by local controllers that receive local data and are usually able to communicate with other local controllers. However, Fully centralized control approach requires massive communication abilities, which makes it infeasible especially in microgrids that cover large geographical areas. Likewise, The extensive interconnection between the units and components of microgrids makes it difficult for fully decentralized control approaches to achieve the minimum coordination needed between different units for efficient control of microgrids.

Considering the arguments mentioned above, the compromising between the two approaches is reasonable, and it is usually performed using hierarchical control scheme composed of three control levels: primary, secondary and tertiary control [19].

Primary control level is at the level of microsources and loads. Mainly, it is responsible for islanding detection, power-sharing monitoring and output control where the output voltage,

11

current, active and reactive power are controlled to ensure meeting the setpoints decided from the secondary level control and damping any oscillations which are usually done by power electronic devices, mainly power inverters.

The secondary control level is referred to as EMS which is responsible for coordinating the operation between energy sources. This is done by setting optimal generation set points based on the equipment status, technical constraints and forecasts of the load demand and renewable DGs power output to ensure generation and demand balance in the microgrid. The solution of EMS scheduling problem is usually attained by either real-time optimization, expert systems or decentralized hierarchical control. EMS approaches can also be categorized according to the control architecture again, to centralized and decentralized approaches. In the centralized approach, the decision of the micro resources setpoints is made in one single central controller to meet a defined objective for the microgrid as a whole. While in decentralized approaches each microsource is considered as an individual smart agent, and it allows the coordination between them to facilitate achieving objectives for both individual local agent and microgrid as a whole. Finally, Tertiary control is responsible for the coordination between a number microgrids and the main utility grid, i.e., controlling the energy exchange between them.

EMS for microgrids and hybrid distributed generation system is a traditional topic that is studied extensively in the literature. It has to meet the short-term energy balance, and long-term energy management which is usually formulated is an optimization problem with an objective of minimizing the cost of supplying the demand. This optimization problem is subjected to many constraints including system reliability and technical limitations of its components where the required solution is usually the unit commitment and dispatch of

DGs. It is worth mentioning that the optimal solution is not always achievable, this is inherited from the nonlinearity of the problem. However, an acceptable optimal or near optimal solution is intended to maximize or minimize specific parameters, and it must satisfy the constraints.

The optimization problem is mainly solved mathematically using mathematical layouts such as linear programming, nonlinear programming, dynamic programming [20] and mixed integer linear programming [21]. The artificial intelligence techniques can also be applied in this case such as particle swarm [22], genetic algorithm [23], ant colony and bee colony optimization techniques.

Essentially, EMS can be categorized in terms of control architecture into three forms of control approaches, centralized, decentralized and hybrid control strategies. Centralized EMS is responsible for attaining energy balance for all connected microgrids to the system [24][25]. Centralized EMSs are suitable for systems that belong to one owner, and they return the best value in terms of operational cost (global optimization). However, they require vast communication infrastructure, higher computational power devices, and offer a limited plug-and-play functionality.

Decentralized EMS deals with each microgrid as an individual entity [26]. Each microgrid has a local EMS that is only responsible for optimizing the operation of local resources. Each of the microgrids may have different objectives and belong to different owners, and in some cases, local EMSs are given the ability to communicate with each other. Although the computational burden is distributed among the EMSs, the decided schedule of the generation resources is not optimum regarding the operational cost.

13

The control in Hybrid EMS is usually composed of two levels: Microgrids local EMSs and MMG system central EMS [27] [28]. Local EMSs optimize local resources in each microgrid at first then they inform central EMS the amount deficit and surplus power rach microgrid need or can provide, respectively. Following, central EMS manage the power transactions between the microgrids and the power trading with the main grid. Hybrid EMS introduced as evolved control approch of centralized and decentrlized as a trade-off EMS. For example, Hybrid EMS give provide flexibility in plug-and-play fuctionality and reduction in operational cost as it compared to centralized EMS and decentrlaized EMS, respictivly.

2.2.2 Microgrids Load Restoration and System Resliency Enhancment

Microgrid, as a source of resiliency and operational support to the power system, has been studied extensively in the literature. The feasibility of a microgrid to serve as a resiliency source is studied in [29]. Three configurations of deployment of a microgrid as resiliency source were considered namely, as a local source, community source, and black start source. The microgrids deployed as local resources, operate to ensure a continuous interruptible power service for local consumers inside their boundary. As a community resource, the microgrids utilize their unused resources to restore interrupted loads outside their boundary, hence, enhancing the resiliency of the whole system. As a black start resource, the microgrids are made to help in the black start of main generation units of the main grid.

In [30] and [31], the microgrids are used to support the resiliency of the main grid by participating in restoring the interrupted loads outside their boundary. A multi-level load restoration scheme is proposed in [30], where the generation capabilities of microgrids and

Electric Vehicles (EV)s are used to enhance the reliability and resiliency of the system after contingencies. In [30], a resiliency-based service restoration approach, dealing with catastrophic outages caused by main disasters, is suggested. Also, the dynamic performance of a distributed generation and microgrid stability is considered. Limits on frequency deviation, transient currents, and voltages incorporated as constraints. Reference [32] mainly constructs management functionalities to manage charging and discharging processes of ESS in microgrids, and to send controlling signals for responsive loads including EVs. The main objective is to enhance the resiliency of the microgrid following islanding event. A resiliency-based microgrid operational control framework is proposed in [2] with an objective of enhancing resiliency by minimizing load curtailment after contingencies. Both grid-connected and islanded operation are considered. The grid-connected operation is modeled as a mixed integer linear programming problem, while islanded mode is modeled as a linear programming problem. The uncertainty of renewable generation resources and loads are considered by using robust optimization strategies. Adjustable loads with pre-defined start and end times are used in load modeling.

In [33], authors focused on utilizing demand-side management to restore a microgrid during an outage, they proposed a demand management mechanism where they classified the loads into interruptible and critical loads. The behavior of the microgrid during the outage is reflected by a proposed new metric "grid autonomy factor". An energy management system for enhancing the resiliency of microgrids on islanded operation is proposed in [34]. A stochastic nonlinear programming optimization problem is formulated with an objective of minimizing the number of unserved loads, which in turn are categorized based on priority into critical and non-critical. The uncertainty in the renewable

resources output power is explicitly considered and the demand response is achieved through adjustable loads and PHEVs.

[35] proposed a rule-based outage management algorithm for restoring microgrids working in islanded mode. The models of the PVs, wind turbines and energy storage were provided, and the generation of the renewable DGs and the demand power were forecasted based on real collected data. Rule-based power management system is faster in execution than power management system based on optimization techniques. However, the rule-based power management system loses effectiveness if the number of components of the microgrid increased and when the microgrid has plug-and-play operation features. [36], [37] and [38] explore the role of EVs parking lots in enhancing the resilience of microgrids where each parking lot is dealt with as an individual distributed ESS that can be used during outage restoration.

According to the IEEE Standard 1547.4 [39], splitting the power distribution system into interconnected microgrids can improve the resiliency and operation of the power system. Networking of microgrids as an upgraded microgrid form and more beneficial way to enhance the resiliency of the power system during contingences is studied in the literature concerning both structure and operation. [40] investigates and presents how two connected islanded microgrids can support each other during contingencies. Microgrids are connected through back to back converter, nominally, each microgrid supplies its local loads autonomously. When an overloading is detected in one of the microgrids, power support is offered by the other. Transformative architecture is proposed in [41], where microgrids that unable to fully supply their local load broadcast requests supply support from other normally operating microgrids. The power transaction from normally operating

microgrids to on-emergency microgrids is controlled through a devised average consensus algorithm in a decentralized manner.

Privacy-preserving energy management algorithm for networked microgrids system for both islanded and grid-connected modes of operation is introduced in [42]. Microgrids are nested to inner and outer levels based on load priorities. The enhancement of system resiliency is the main objective in islanded operation, and this is achieved by enabling disconnected microgrids to form subgroups. Authors in [43] propose an outage restoration technique for power systems after natural disasters. The grid is sectionalized into self-adequate multiple microgrids which are coordinated to restore critical loads by formulating MILP optimization problem. A careful review of the related literature suggests that more effort should be put to study the issue of how multi-microgrid systems should respond to survive catastrophic outage by both coordinating local resources and applying suitable demand response program.

2.3   Demand Side Management (DSM)

Conventionally, the energy management of microgrid usually concerned with the scheduling of the DGs, but recently the flexibility of the local loads of the microgrid incorporated to the energy management problem using DSM programs. DSM programs can be defined as the set of measures that are planned to be performed on the consumption side to improve the overall efficiency, reliability, and security of the power system. The typical objectives of DSM programs are the reduction of the total energy consumed in the power system, the minimization of the capacity and size of system infrastructure needed to

17

supply the energy demand needs and the rescheduling of the consumption to match the generation especially in renewable DG based power systems [44]. DSM rely mainly on two aspects energy efficiency measures and demand response measures [45]. Energy efficiency measures are all the changes and improvements done on characteristics and the physical properties of the system. For example, providing better insulation on buildings reduces energy consumption needed to raise or lower the room's temperature. On the other hand, DR refers to the measures performed to alter the consumption behavior of the end-users to meet certain objectives usually in response to electricity pricing or the availability of power generation. This study concerned on DR and from now on it will be referred to as DSM. DSM programs are realized by two methods shedding and/or load shifting. The first method is to reduce the consumption of a certain load, while in the second the consumption is shifted and rescheduled to another time with lower electricity prices or when an excess renewable power is available.

DSM programs can be categorized into incentive-based and time-based [46] [47]. In incentive-based programs, participants are paid to change their consumption behavior. Those programs are also called direct DSM programs as the power system operator given permissions from customers to decide the shape of consumption usually based on contracts. Direct Load Control (DLC) [48], interruptible/ curtailable rate (I/C) [49], emergency demand response [50] and demand bidding [51] schemes are some examples of incentive-based DSM programs. Participants on DLC DR agree to grant the utility the ability to remotely control the operation of certain devices by installing remotely controlled switches. The utility will have a complete control on the on/off status of these devices and in return discount rates or agreed payments is given to the participants. Unlike DLC

program which is usually adopted for small residential loads, I/C programs are more suitable for large industrial customers who are usually asked to curtail a certain part of their electric load or to reduce the overall consumption to a certain level upon notice. In such program, participants are rewarded if they comply, but they are also penalized if they failed to reduce their consumption to the required level. Participants in emergency demand response benefit incentive payments and discount rates by agreeing to be in call to reduce their energy consumption whenever needed during emergencies. Finally, demand bidding programs depend on the bids made by participants. In this program, participants, usually large consumers, bid the price of the amount of load curtailment they can perform or the price of power consumption they are willing to pay. Once an agreement is reached participants must fulfill their bids otherwise they will be penalized.

On the other hand, time-based DSM programs provide the customers with the electricity prices for different use times. In such programs, customers respond to the changing rates of electricity pricing to save costs without the direct intervention of the program operator. The pricing of electricity usage can be predetermined where usually a day ahead pricing schedule is generated or dynamic where real-time pricing is provided to the customers. Time of Use (TOU) [52], Critical Peak Pricing (CPP) [53] and Real Time Pricing (RTP) [54] schemes are typical examples of time-based DSM programs. In TOU tariff scheme, the prices are set by the utility for different time periods. These time period are usually categorized into peak period, mid-peak period and off-peak period. CPP program is very similar to TOU program except that the price of use during at least on period, usually peak period, can change regularly or in accordance to the status of the system. Finally, the

pricing of the periods in RTP program is announced in a rolling biases where the price of

the next time period is announced before it begins in a short time.

CHAPTER 3

Microgrid System Components and Modeling

This chapter briefly discusses the main components of microgrid and presents their mathematical modeling that is needed for the development of the restoration technique. This chapter specifically elaborates on renewable DG, i.e. photovoltaic (PV) generators and wind turbines, ESS and loads.

3.1   Distributed Generators

DGs are small-scale generation units as they compared to utility central generation stations. DG supply microgrids with energy generated from various primary resources, those resources can be categorized into renewable and non-renewable (conventional) resources. Those DGs are usually classified by the energy management agents into dispatchable and non-dispatchable generation units, respectively [55]. The output power of non-renewable (conventional) DGs is controlled externally by set points while renewable DGs output power is typically controlled following the optimum operating condition of their primary resources. The deployment of DGs in power systems is trending worldwide especially renewable DG with an expected average increase of (2.4%/year) between 2015 and 2040 [56]. For example, Germany is planning to be able to produce half (50%) of the country total power generation from renewable resources by the year of 2050 [57]. PV generators,

wind turbines and conventional fuel-based generators that are assumed to be of the building components of the microgrids considered in this thesis are illustrated next.

3.1.1 PV Generators

The rate of deployment of PV systems as prime renewable energy generators is raising dramatically worldwide. This world-wide raise is estimated by at least 50 GW and 74.4 GW in 2015 and 2016, respectively [58]. This substantial increase is due to the solid advantages offered by PV systems such as:

1- No fuel cost, as they directly consume the energy received from the sun by the photovoltaic effect [59].

2- Low maintenance cost, as the power generation concept does not require moving parts.

3- Simple expandability, by connecting more parallel or series PV modules [60].

4- Flexible installation location, as they are usually designed to indure rigid surrounding conditions.

5- Environmentally friendly, as they produce no noise or carbon emissions.

Solar cells are considered as the fundamental building unit of the PV arrays where they are connected in series to form a PV module, or panel, which are connected also in parallel and series to form a PV array as shown in Figure 3.1 [61]. Considering the PV layout, connecting the modules in parallel determines the voltage level while connecting them in series defines the output current.
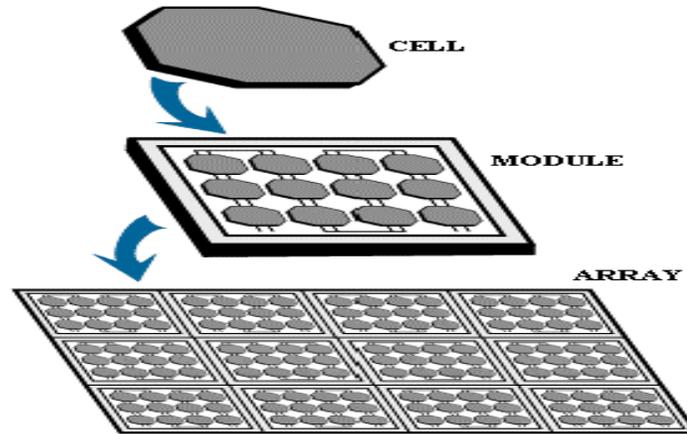
Figure 3.1 PV Array Composition [62]

Solar cells can be categorized based on their composition into silicon PV cells, non-silicon (PV) cells, organic (PV), and film (PV) cells. The most chemical element used in PV cells manufacturing is Silicon. The typical commercial Silicon PV cell types are Mono-Crystalline cells (The most efficient but the most expensive), Poly-Crystalline cells (Less efficient but cheaper) and Amorphous cells (The least efficient but the cheapest, most flexible and most portable) [63].

Regardless of the semiconductor material used in manufacturing PV cells, the working principle is the same for all types and it mainly relies on the photovoltaic effect. As shown in Figure 3.2, when solar light beam strikes the surface of the PV cell, semiconductor material absorbs a fraction of the energy of the photons in this beam. This has the potential to release outer electrons allowing them to flow freely in the silicon lattice. The electric field produced by interfacing the P-type substrate (negative layer) and the N-type substrate (positive layer) forces the freed electrons to flow in a certain direction when a connection is made between the two layers.

23
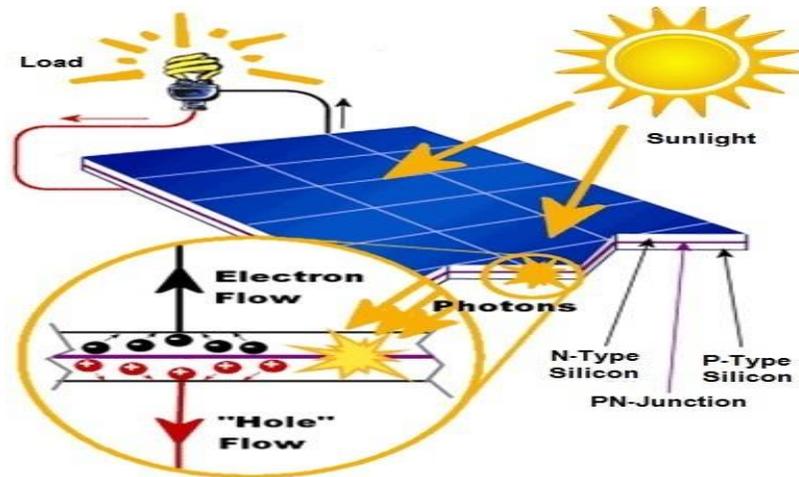
Figure 3.2 Operating Principle of PV Cell [64]

The equivalent electrical circuit model of ideal PV cells is represented as a current source that represents the photo-generated current in parallel with a diode which depicts the P-N junction of the solar cell as shown in Figure 3.3.
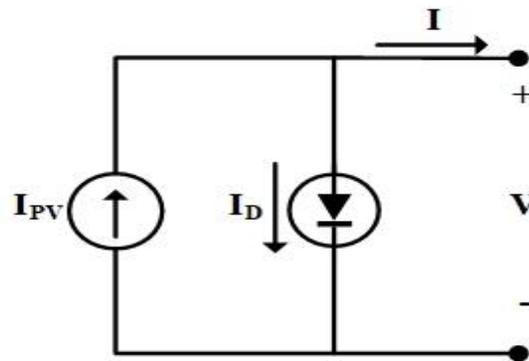
Figure 3.3 Equivalent Electrical Circuit of Ideal PV Cell

More practical models have been used in literature mainly single diode and double-diode models in where an additional parallel and/or series resistor added to the ideal PV cell model [65-67]. Those extra resistors are usually added to account for leakage current through the cell and the losses of semiconductor material itself. The governing equations of the ideal PV model are as follow [68]:

$$I = I_{ph} - I_d \tag{3.1}$$

$$I_d = I_0 * \left[e^{\frac{V}{V_t * A}} - 1 \right] \tag{3.2}$$

$$V_t = k * \frac{T_c}{q} \tag{3.3}$$

Where:

I: is the PV cell output power [A]

I_{ph}:   is the photo-generated current [A]

I_d: is the diode current [A]

I_0:   is the PV cell reverse saturation current [A]

V: is the PV cell terminal voltage [V]

A: is the ideality factor which depends on the PV cell technology

V_t: is the thermal voltage [V]

T_c: is the cell temperature [K]

k: is Boltzmann constant ($1.381 * 10^{-23}$) [J/K]

q: is electron charge ($1.602 * 10^{-19}$) [C]

As it can be deduced from the mathematical governing equations of ideal PV cell model, the relation between the terminal voltage and output current is nonlinear. The voltage and current characteristics of PV cells is usually described by I-V PV curve. The typical shape of I-V curve of an illuminated PV cell is depicted in Figure 3.4. PV cell produces the

maximum current when no resistance is connected between its terminal and this current is called as the short circuit current abbreviated as (I_{SC}). This current is produced when the PV cell is shorted, and the terminal voltage equals zero. On the other hand, the maximum voltage occurs when the cell is open circuited, this voltage known is open circuit voltage (V_{OC}), and the current at this point equals zero because the connected resistance is infinitely high. The power produced by the PV cell can be calculated simply by multiplying the voltage by the current. The maximum power available from PV cell occurs at a certain maximum power point voltage (V_{mp}) and current (I_{mp}).
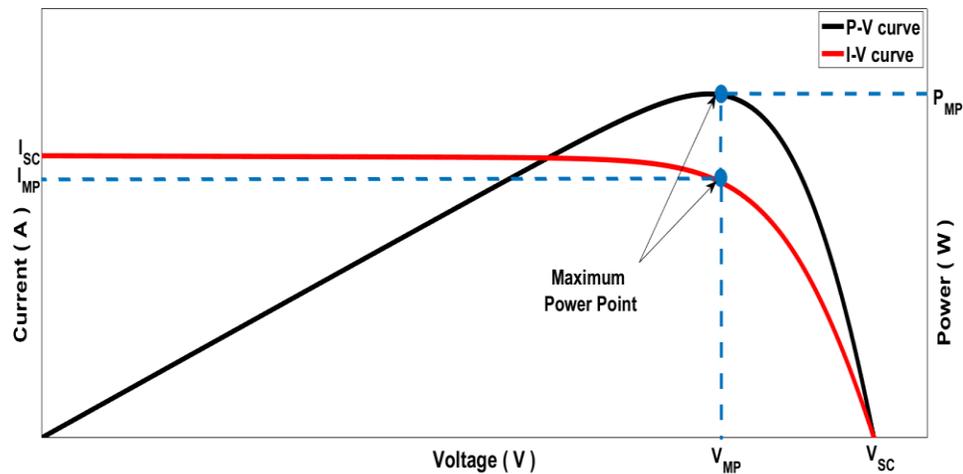
Figure 3.4 Typical IV Characteristics of PV Array

The ability to forecast the output of the PV system is crucial in both planning and operation stages. In literature, there are basically two types of modeling which mainly consider the output power or the output energy over a certain period. Modeling the output power is usually done by using either statistical or historical data to derive models based on regression analysis or by translating the output at certain reference conditions to another set of conditions [69-72].

26

PV system output power is affected by surrounding conditions especially solar irradiance and ambient temperature. The short circuit current of the PV cell is directly proportional to the level of solar irradiance hence output power is also directly proportional to the level of solar irradiance. In the other side, as the ambient temperature increases the open circuit voltage the PV cell drops. In other words, the output power of PV array is inversely proportional to the ambient temperature. Figure 3.5 shows the relation between P-V curve and the variance in solar irradiance level and ambient temperature.
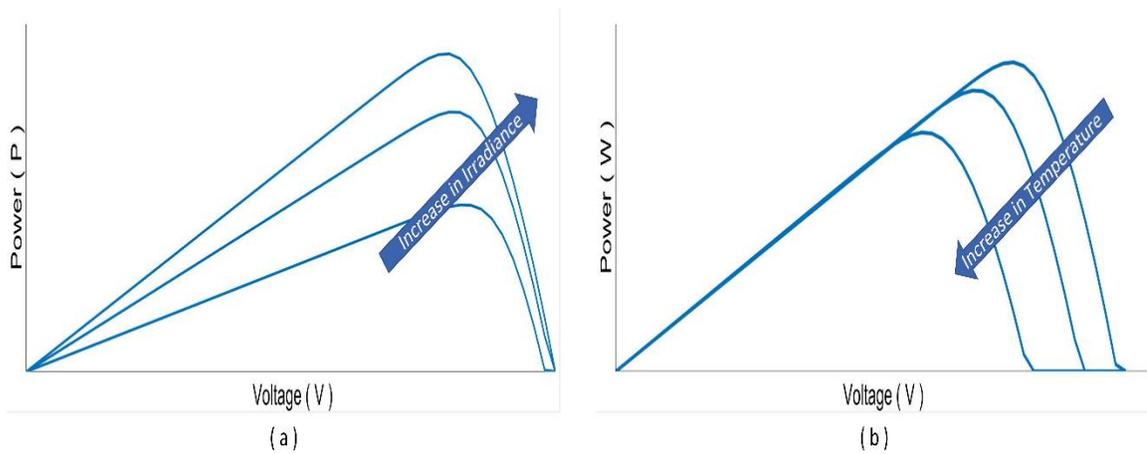
Figure 3.5 Typical PV Array P-V Characteristics under Different (a) Solar Irradiance Level (b) Ambient Temperature

In this study a mathematical model is used to describe the maximum power output of PV system [73]. This model takes the solar irradiation and ambient temperature inputs and make use of the I-V curve and data given by the PV system manufacturer to predict the output power.

I-V characteristics of the (PV) system is calculated by:

$$I = S * [I_{SC} + K_I(T_C - 25)] \qquad (3.4)$$

$$V = V_{OC} - K_V T_C \tag{3.5}$$

I $[A]$ and V $[V]$ are the voltage and the current of the solar PV module. S denotes the level of solar irradiance measured in $[KW/m^2]$. K_I $[A/C^o]$ is the short circuit current temperature factor and K_V $[A/C^o]$ is the open circuit voltage temperature factor and they both are provided by the manufacturer. I_{SC} $[A]$ and V_{OC} $[V]$ are the short circuit current and open circuit voltage measured at standard test conditions (STC), respectively and they both are provided by the manufacturer. T_C $[C^o]$ is the solar cell operating temperature and it can be calculated as follows:

$$T_C = T_A + \frac{S * (N_{OT} - 20)}{0.8} \tag{3.6}$$

T_A (C^o) is the ambient temperature and N_{OT} (C^o) is the PV cell nominal temperature of operation which is also provided by the manufacturer. The output power of the PV system can be calculated using the following relation:

$$P = N * FF * V * I \tag{3.7}$$

N is the number of connected PV modules. FF refers to the fill factor which is one key parameter in determining the maximum output power and is used as an indicator for the PV system performance and its calculated as follows:

$$FF = \frac{V_{MP}\, I_{MP}}{V_{OC}\, I_{SC}} \tag{3.8}$$

V_{MP} $[V]$ and I_{MP} $[A]$ are the voltage and the current recorded at the maximum output power, respectively. The STC usually are 0.8 $[KW/m^2]$ solar radiation and an ambient temperature of 25 $[C^o]$.

3.1.2 Wind Turbine Generators

The use of wind energy expanded tremendously in the last decade as it recognized as an environment-friendly and cost-efficient alternative energy source. According to International Renewable Energy Agency (IRENA), wind generation accounts for the second largest share (23%) of renewable generation capacity with an estimated installed capacity of 467 GW [74]. Wind generation systems are composed mainly of three parts wind turbine, generator, and control system. The wind turbine consists of a rotor of two or more blades placed at a hub that is mounted on a nacelle and a tower. Wind turbines mainly exist in two configurations vertical axis wind turbines and horizontal access wind turbines. The turbine is connected to the shaft of the generator through a gearbox which converts the rotational speed from the turbine to a higher desired rotational speed of the generator. The main types of generators implemented in wind generation systems are Doubly-Fed Induction Generator (DFIG), Synchronous Generators (SG) and Induction Generators (IG). Finally, the control system is responsible for maintaining the power output generated by the rotation of the generator shaft at a certain level. The main equation that describes the active output power of the wind generation system is given by [75]:

$$P = \frac{1}{2} * \left(\rho * A * V^3 * C_p \right) \tag{3.9}$$

Where :

P: is the output active power $[W]$

ρ: is the air density $[\frac{kg}{m^3}]$

V: is the wind speed $[\frac{m}{sec}]$

29

A: is the rotor area [m^3]

C_p: is the power coefficient

Power coefficient is the ratio of the output power of the wind generator over the kinetic power of the wind rotating the rotor. In other words, it can be regarded as the efficiency of the wind generator, and it mainly depends on the aerodynamics and transmission efficiency of the wind turbine.

The output power of wind generators depends principally on three factors. The first factor is the power curve of the wind generator itself which depends in turn on many parameters such as the efficiency of mechanical transmission and electricity converting and the aerodynamics of the wind turbine design. The second factor is the wind speed profile of the installation location, as the wind speed has a direct relation to the output power of the wind generator. The last parameter is the height of the wind generator hub, and this due to the fact that the wind speed increases with altitude.

In this study, the hourly wind speed is simulated by means of Weibull distribution function shown in equation (3.10) and the estimated hourly wind speed is obtained using equation (3.11):

$$F_v = 1 - exp\left(-\left(\frac{V}{c}\right)^\sigma\right) \tag{3.10}$$

$$V = c\left[-ln(r)\right]^\sigma \tag{3.11}$$

Where F_v is the cumulative distribution function of Weibull distribution and V represents the wind speed. σ and c are the shape and scale factors, respectively. r is a random number

between 0 and 1 generated by uniform distribution. The values of σ and c differ from a location to another and they are calculated based on historical data of wind speed.

Different wind generators have different output power curves. As a result, the modeling of the output power is also different from one wind generator to another. A typical wind generator power curve is shown in Figure 3.6.
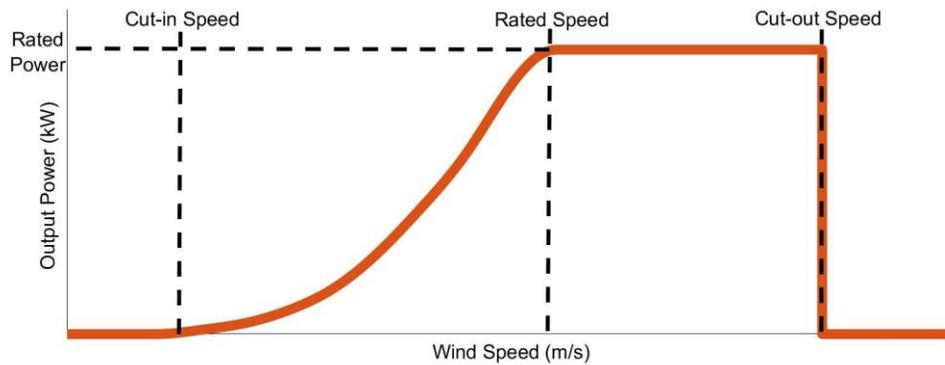
Figure 3.6 Typical Shape of Power Curve of Wind Generator

At low wind speed, there is no sufficient exerted torque on the wind turbine rotor blades to move. As the wind speed increases the exerted torque on the wind generator rotor increases and it will start to rotate after a sufficient torque is applied. Cut-in speed is the minimum wind speed that can apply enough torque to rotate the wind turbine rotor. As the wind speed increase over the cut in speed the output power also starts to increase until it reaches the maximum power level the wind generator capable of producing. This power is regarded as the rated power of the wind generator and is achieved at a corresponding rated wind speed. The rated power level is then maintained until the wind speed gets over the cut-out speed. When the cut-out wind speed is reached the power, generator is made to stop operating.

In this study, the characteristic equation of the output power is obtained by fitting the practical power curve given by the manufacturer using cubic spline interpolation. The fitting equation of the output power of the wind generator is as follows [76]:

$$P_W(V) = \begin{cases} 0 & V \le V_{cin} \quad or \quad V \ge V_{co} \\ a_1 (V - V_{cin})^3 + b_1 (V - V_{cin})^2 + c_1 (V - V_{cin}) + d_1 & V_{ci} < V < V_1 \\ a_2 (V - V_1)^3 + b_2 (V - V_1)^2 + c_2 (V - V_1) + d_2 & V_1 < V < V_2 \\ . \\ . \\ . \\ a_n (V - V_{n-1})^3 + b_n (V - V_{n-1})^2 + c_n (V - V_{n-1}) + d_n & V_{n-1} < V < V_r \\ P_r & V_r \le V < V_{co} \end{cases}$$

(3.12)

Where P_W is the output power [W] at wind speed V [m/s] at the hub height. V_{cin}, V_{co} and V_r are the cut in speed, cut out speed and the rated speed, respectively; P_r is the rated output power. n is the number of cubic spline functions that is calculated based on n+1 break points given by the manufacturer. Finally, a,b,c and d are the coefficients of the cubic polynomials of the interpolation.

Because wind speed is not constant with altitude. Wind speed profile has to be adjusted the height of the wind generator hub. In this study the wind speed profile is adjusted by using Hellmann exponential law [77]:

$$V = V_0 \left(\frac{h}{h_0} \right)^\alpha$$

(3.13)

Where:

V: is the wind speed at the wind generator hub $[\frac{m}{s}]$

V_0 is the reference wind speed at the anemometer height $[\frac{m}{s}]$

h: is the height of the wind generator hub $[m]$

h_0:   is the reference height of the anemometer $[m]$

α: is the power law exponent

The power law exponent is not constant for certain location and it is affected by many parameters such as the time of the day, the season, the nature of the terrain, the wind speed and the temperature. However, typical values ranging usually between 0.1 to 0.7 is used in literature for the power law exponent. Those values determined is conventionally according to the topography of the installation location [77].

3.1.3 Conventional Generators Modeling

Conventional generators are usually electromechanically driven in which they convert mechanical energy generated by fuel combustion most commonly natural gas or diesel fuels into electrical energy. Conventional generators can work as the primary source to supply the demand of the microgrids. However, they are more commonly used as a pack up energy sources when the when renewable DG and ESS integrated to the microgrid cannot serve the load demand.

Diesel generators are the most commonly used conventional DG in microgrids, and they considered in this study to serve as dispatchable backup generation units. Those units will be dispatched when the generation when renewable cannot meet the load.

The size of the diesel generator engine mainly depends on the rated power they can generate. The fuel consumption is usually modeled in literature as a quadratic or linear function of the dispatched power [78] [79].

Linear fuel consumption of diesel generators is adopted in this study as described by the following equation:

$$F = a.P + b \qquad\qquad (3.14)$$

F is the hourly fuel consumption of the diesel generator. P is the dispatched output power of the diesel generator. Finally, a and b are the fuel consumption constant of the diesel generator.

In addition, technical constraints is also considered in the mathematical modeling of the diesel generator including maximum Up/Down ramps, minimum up/down operating times and minimum output generation as it will be presented in section (4.4).

3.2   Energy Storage System (ESS)

Considering the intermittent nature of the output of renewable generators, installing ESSs to the microgrid is curial as they not only help in refining the shape of the renewable DGs output but they also help in reducing the operational cost by storing excess energy when the output power from renewables is larger than the demand [80] [81]. The existing energy storage technologies can be classified into two categories. The first category is the direct energy storage technology, where the electric energy is stored directly without converting

it to another form of energy this category includes Superconducting Magnetic Energy Storage (SMES) and Ultra Capacitor Energy Storage (UCES). The other category is the indirect energy storage technologies, where the electrical energy is converted to another type of energy to be stored, most commonly as mechanical and chemical energy. Examples of the indirect energy storage technologies include Battery Energy Storage Systems (BESS) and Flywheel Energy Storage Systems (FESS). The energy storage systems usually described by two characteristics energy density and power density [82]. Energy density is related to the amount of energy that an ESS can store relative to its weight. On the other hand, Power density is associated with the discharge rate of power of the ESS in respect of its weight. The application of implementing ESSs in microgrids are divided to the short-term application and long-term application. First, Short-term applications require ESSs with large discharge power rate (high power density) which able to supply a large amount of energy in short period ranging from a few seconds to a few minutes. Short-term applications are mainly correlated to the support of power quality, security, and reliability of the power system. In the other hand, long-term application of ESSs in microgrids are typically associated with the support of energy generation units DGs. In this type of applications, ESSs are used as a source of energy and to support energy management operations.

Using ESSs in energy management of microgrid requires high energy density capabilities, and the most commonly used ESS technologies in such small or medium scale power networks is BESS especially lead-acid batteries [83]. The prevailing use of the lead-acid in microgrids is because they are well mature technology that provides sufficient acceptable performance with a relatively low cost.

3.2.1 Energy Storage System Modeling

The common practice for operation and management of ESS in the microgrid is to estimate the available energy stored in it. The amount of stored energy is habitually described by a factor known as the State of Charge (SOC). SOC refers to the ratio of the available energy stored over the rated capacity ESS as follows [83]:

$$SOC(t) = \left(\frac{E(t)}{C_{ESS}}\right) * 100 \tag{3.15}$$

Where $E(t)$ is the available stored energy at time t $[Kwh]$, C_{ESS} is the rated storage capacity of the ESS.

The modeling of units of ESSs considered in this study is mainly based on a state transition equation that the describes SOC at each time step [84]:

$$SOC(t+1) = SOC(t) + \left(\frac{\left(P^{ch}(t) * \eta^{ch} - \frac{P^{dch}(t)}{\eta^{dch}}\right) * \Delta t}{C_{ESS}}\right) * 100 \tag{3.16}$$

Where $P^{ch}(t)$ and $P^{dch}(t)$ are the charge and discharge rates of the ESS unit at time measured in $[Kw]$, respectively. Δt is the duration of power charging and discharging $[hour]$. Finally, η^{ch} an η^{dch} are the charging and discharging efficiencies of the ESS.

Constraints on the power rates and the energy stored are also imposed as follow:

$$0 \leq P^{dch} \leq P^{dch,max} \tag{3.17}$$

$$0 \leq P^{ch} \leq P^{ch,max} \tag{3.18}$$

$$SOC^{min} \leq SOC \leq SOC^{max} \qquad\qquad (3.19)$$

Where $P^{dch,max}$ is the maximum discharge rate. $P^{ch,max}$ is the maximum charge rate. Finally, SOC^{min} and SOC^{max} represents the maximum and minimum amount of energy stored in the ESS.

3.3   Loads

Load profile can be defined as the shape of energy consumption amount over time. Many factors affect the shape of the load profile. Those factors include social and environmental changes. For example, User types, holidays seasons, entertainment events and temperature. User types are usually categorized into residential, commercial and industrial types [85].

In this study typical residential and commercial load profiles are considered. Loads are classified based on supply priority into three levels high priority, medium priority and low priority loads. Higher priority loads require high quality continuous power supply, while lower loads can be shed or interrupted to insure supply to higher priority level loads. Furthermore, part of the loads is considered to be shiftable. This type of loads can be shifted to different use time and this load shifting process is decided in accordance to different constrains such as the availability of energy generation and customer preferences. shiftable loads mostly of residential type and their examples include dryer and washing machines, cooling devices and EVs.

DSM is incorporated into the load restoration technique developed in this study by realizing a load shifting and shedding schemes. Firstly, preemptive load shifting signals are

produced as the first step of the restoration technique. The consumption of certain loads rescheduled according to the forecasted generation and load consumption patterns to reduce the overall load shedding during the contingencies. Secondly, emergency load shedding is facilitated by prioritizing the loads into high priority, medium priority and low priority loads. During emergencies, lower priority loads are the first to shed whenever needed in favor of higher priority loads to be supplied. The mathematical modeling of incorporating the adopted DSM schemes will be represented in chapter 4.

CHAPTER 4

PROBLEM FORMULATION

This chapter will introduce and address the main problem, as well as provide an overview of the distribution systems architecture and control framework. Furthermore, this chapter includes a brief introduction of mathematical optimization along with the technique used in this study. Finally, the stages of the proposed load restoration technique will be illustrated, with their mathematical formulation shown.

4.1   Problem Description

Power system contingencies may cause outages that cover wide area. Large number of customer may be affected and lose their power supply, especially when crucial power system components such as overhead lines. Microgrids in response, isolate themselves from the faulty portions of the power system and operate on islanded mode. In islanded mode operation, power service is sustained by optimally scheduling local resources and flexible loads. This ability of islanded microgrids to sustain an acceptable level of service without the reliance on the main utility central generation units and long transmission paths makes them more immune to such contingencies. Moreover, applying load restoration measures on microgrids is much faster and easier than apply them to the large-scale utility grid. This stems from the fact that microgrids installed generation capacity is normally less

than 10 MVA and that the load restoration measures designed for microgrids are formulated to cover a smaller generation and demand balancing areas [31].

In this context, the division of power system load into smaller portions wherein each portion is supplied by one microgrid will enhance the immunity of the distribution system against contingencies. By applying such a load division, the distribution system is thus composed of a number of networked microgrids, otherwise known in this study as the MMG distribution system. The main objective of this study is to propose a load restoration technique that can be applied on MMG distribution systems, which isolate from the main grid after a contingency is detected. Each microgrid is connected to the rest of the distribution system through the PCC and is composed of multiple conventional and renewable DGs, ESSs and controllable and non-controllable loads, as shown in Figure 4.1. The term "controllable loads" refers to the loads that can be shed or shifted if needed.
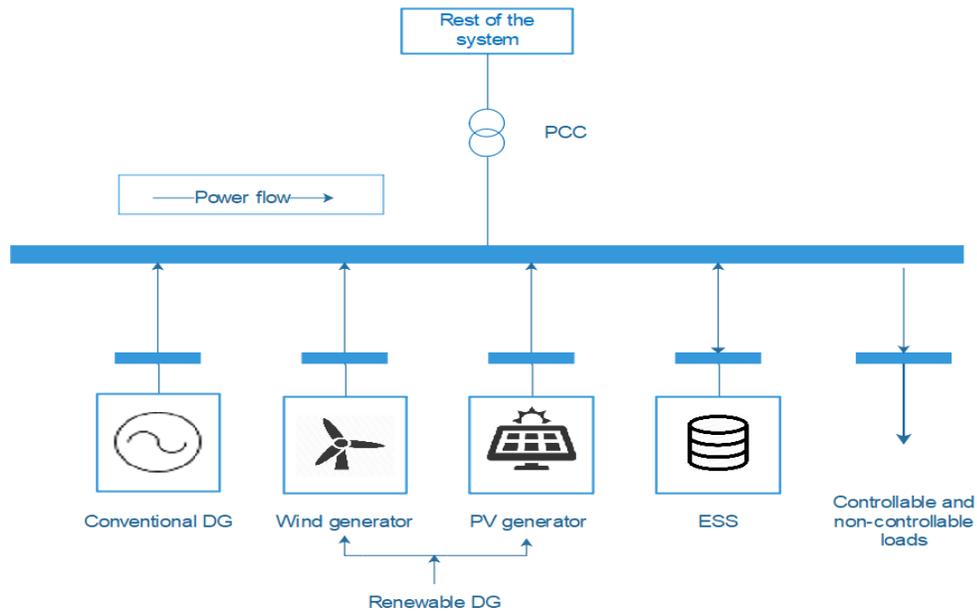
Figure 4.1 Schematic of Microgrid

The proposed operational and control framework of the MMG distribution system is depicted in Figure 4.2. A hierarchical control framework consisting of three levels of control was adopted for this study. In the control framework, lower level control agents receive commands from the upper levels, yet the latter base their decisions on collected data from lower-level control agents.
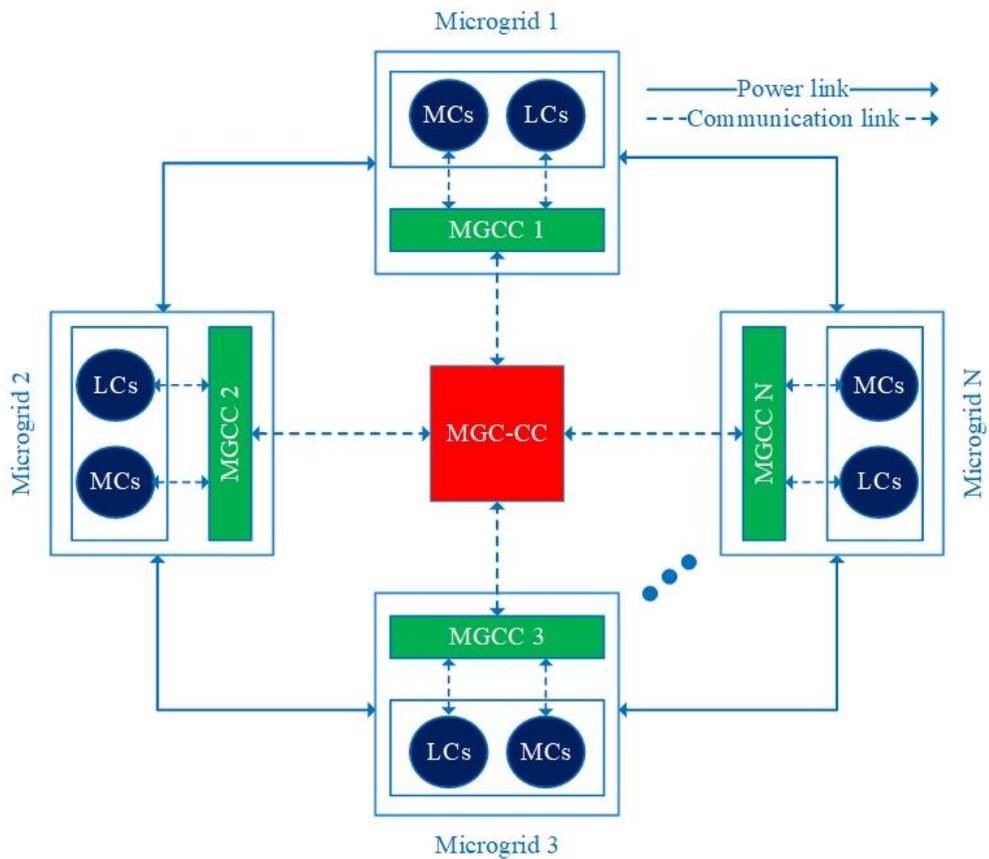
Figure 4.2 MMG System Control and Operational Framework

The first control level is the lowest level, consisting of two types of control agents, namely local micro-source controllers (MCs) and local load controllers (LCs). The second control level is composed of one agent, the microgrid controller (MGC). Finally, the third control level is the highest level, otherwise known as the microgrid community central controller

(MGC-CC). The rules and responsibilities of each control agent are as follows:

A. Level I (MC and LC):

LCs are responsible for setting the on/off state of associated load points, based on the command signals produced by the MGC. MCs, on the other hand, are responsible for ensuring the generation power issued by the MGC from the DGs locally installed in the microgrid while keeping the voltage and frequency of the microgrid within acceptable limits. LCs and MCs are also responsible for providing the MGC with the forecasted demand and renewable DGs output power.

B. Level II (MGC):

MGC is responsible for scheduling the local resources and loads of the microgrid, as well as producing control signals to level I controllers. Scheduling is based on the forecasted information received from level I controllers. Additionally, MGC collects data pertaining to the deficit or surplus amount of power inside the microgrid and sends it to the MGC-CC.

C. Level III (MGC-CC):

MGC-CC is the highest level of control and is responsible for optimizing the power transactions between microgrids comprising the MMG system. Power transaction is determined by the data received from MGCs. Once the power transactions are determined, MGC-CC sends signals to MGCs to update the generation schedule.

4.2 Mathematical Optimization

Mathematical optimization is the selection process of the best element from a set of available alternatives that are all subjected and satisfy specific constraints. Optimization problems are usually developed to minimize or maximize a certain function. For example, the optimization problem can be developed to minimize the cost or to maximize the benefit. Optimization problems consist of the following three parts: the objective function (the deciding criterion), the constraints, and the decision variables. Mathematical optimization problems are classified according to the nature of the objective function and the constraints to linear, integer, mixed integer linear and nonlinear. Hence, mathematical programming can be classified into the following categories: linear programming (LP), integer programming (IP), mixed integer linear programming (MILP) and mixed integer nonlinear programming (MINLP), among others. These mathematical programming types can be similar, and solving techniques used in one type can be employed by another. For instance, LP forms the basis of MILP where the main difference lies in the decision variables that present only integers rather than real numbers in MILP. LP solvers typically use simplex or interior point techniques, while branch- and bound-based techniques are most commonly used techniques in MILP alongside those used in LP [86-88]. In this study, the optimization problems included in the proposed restoration technique namely, the problems of the generation of preemptive load shifting signals, the individual microgrid local resources scheduling, and the global optimization of the MMG system are formulated as MILP optimization problems.

4.2.1 Mixed Integer Linear Programming (MILP)

In MILP, all the objective functions and constraints are linear. The decision variable can pose both real and integer values where an additional non-negativity constraint can be added to ensure the valued decision variables are positive. In addition, integer decision variables can be restricted to values of zero or one to replicate binary decisions.

The typical form of n real decision variables, m integer decision variable, one objective function, p equality constraints and q inequality constraints MILP optimization problem is expressed as follows:

$$Min_{(x,\delta)} \; \boldsymbol{C_x}^T \boldsymbol{x} + \boldsymbol{C_\delta}^T \boldsymbol{\delta} \tag{4.1}$$

$$\boldsymbol{A_x}\boldsymbol{x} + \boldsymbol{A_\delta}\boldsymbol{\delta} \leq \boldsymbol{b} \tag{4.2}$$

$$\boldsymbol{A_{eq,x}}\boldsymbol{x} + \boldsymbol{A_{eq,\delta}}\boldsymbol{\delta} = \boldsymbol{b_{eq}} \tag{4.3}$$

And where:

$\boldsymbol{C_x}$ is the cost matrix of objective function associated with the real-valued decision variables, size $(1 \times n)$;

$\boldsymbol{C_\delta}$ is the cost matrix of objective function associated with the integer-valued decision variables, size $(1 \times m)$;

$\boldsymbol{x}$ is the real-valued decision variables matrix, size $(1 \times n)$;

$\boldsymbol{\delta}$ is the integer-valued decision variables matrix, size $(1 \times m)$;

$\boldsymbol{A_x}$ is the coefficients matrix associated with the real-valued decision variables of q inequality constraints, size $(q \times n)$

$\boldsymbol{A_\delta}$ is the coefficients matrix associated with the integer-valued decision variables of q inequality constraints, size $(q \times m)$

$\boldsymbol{b}$ is the constant matrix of the q equality constraints, size $(q \times 1)$

$\boldsymbol{A_{eq,x}}$ is the coefficients matrix associated with the real-valued decision variables of p equality constraints, size $(p \times n)$;

$\boldsymbol{A_{eq,\delta}}$ is the coefficients matrix associated with the integer-valued decision variables of p equality constraints, size $(p \times m)$; and

$\boldsymbol{b_{eq}}$ is the constant matrix of the q equality constraints, size $(p \times 1)$;

4.3   Development of Load Restoration Technique

The proposed load restoration technique is designed for application on the islanded MMG distribution system when a contingency in the main utility grid is detected. It consists of two stages formulated as MILP optimization problems. In the first stage, the preemptive load shifting DR program is applied to reshape the load profile depending on available resources. The second stage concerns the scheduling of available resources and it is divided into two steps. Firstly, the scheduling of local microgrids resources and controllable loads is done. Secondly, the power transaction between the microgrid is determined. The following is to illustrate the two stages in details:

45

- **First Stage (Preemptive load Shifting DR program):**

The main objective of this stage is to reshape the demand according to the availability of generation and to reduce the shedding of high priority loads. Once an emergency is detected, preemptive load shifting signals are generated for the next T_{shift} time slots in each microgrid by the associated MGC by solving a formulated MILP optimization problem. In addition to the forecasted local resources generation and load demand received from the LCs and MCs, the technical constraints of the system components are considered in the determination of the amount of load shifting at each time step. The load shifting signals then sent to the corresponding LCs by MGC, which are subsequently relayed to the customers.

- **Second Stage (Local and Global Scheduling)**

In the first step of the second stage, each microgrid's MGC schedules the available local resources and determines the amount of the emergency load shedding necessary based on the data it receives from local LCs and MCs. This is done by solving the MILP Rolling Horizon (RH) optimization framework problem, wherein at each slot, the MGC schedules the local resources and controllable loads for a specific period of time (local optimization scheduling horizon, T_{local}). However, it is only the schedule on the following time slot that is considered to be performed next (local optimization scheduling control horizon). Once the schedule of resources and controllable load is determined, the MGCs calculate the surplus and deficit energy for the next time slot inside every microgrid and report the data to the MGC-CC.

The main advantage of the RH optimization strategy is the control of outcome for a particular time slot while considering its successors and maintaining the ability to respond to unforeseen events. Therefore, it provides further flexibility for the proposed load restoration technique. In addition, by adopting the RH optimization strategy, the proposed technique's strength will increase, as it implicitly tolerates the volatility of the forecasted generation. Figure 4.3 depicts the operation of the RH optimization strategy and distinguishes between scheduling and control horizons.
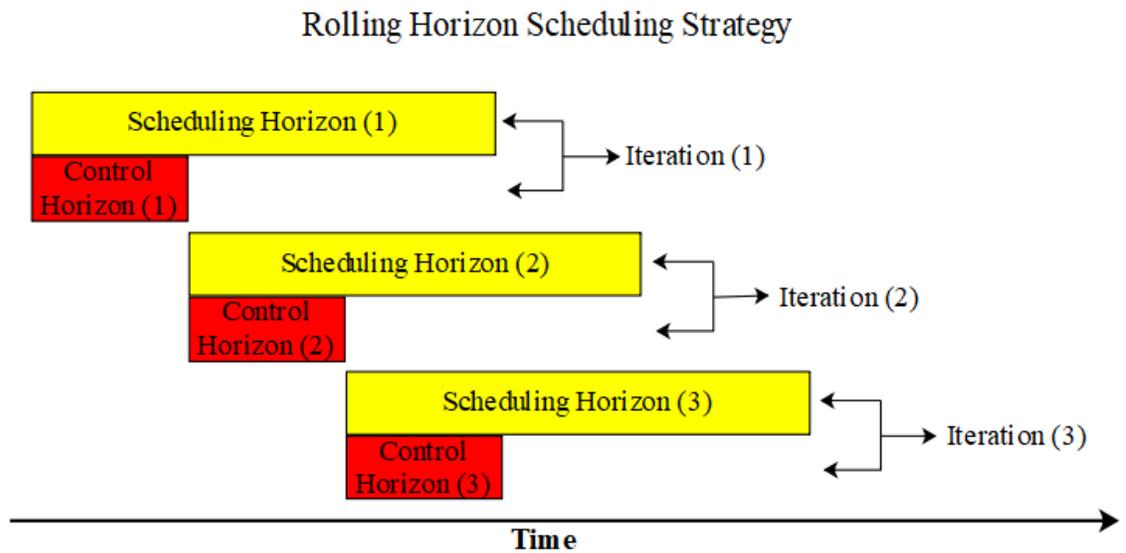
Figure 4.3 Rolling Horizon (RH) Scheduling Strategy Operation

In the next step of the second stage, MGC-CC schedules the power transactions between the microgrids for the following time slot based on the information sent by the MGCs, with the objective of recovering unsupplied loads of the microgrids. Next, both the updated set points for the generation of DGs and the load shedding signal for the current time step are sent to MGCs and corresponding MCs and LCs respectively, who then react accordingly.

47

At the end of each time step, the MGC-CC verifies if the system emergency is cleared. If the system emergency status is still activated, the local optimization is performed again; otherwise, the load restoration technique is terminated. Figure 4.4 summarizes the stages of the proposed the restoration technique and the rules of the control agents.
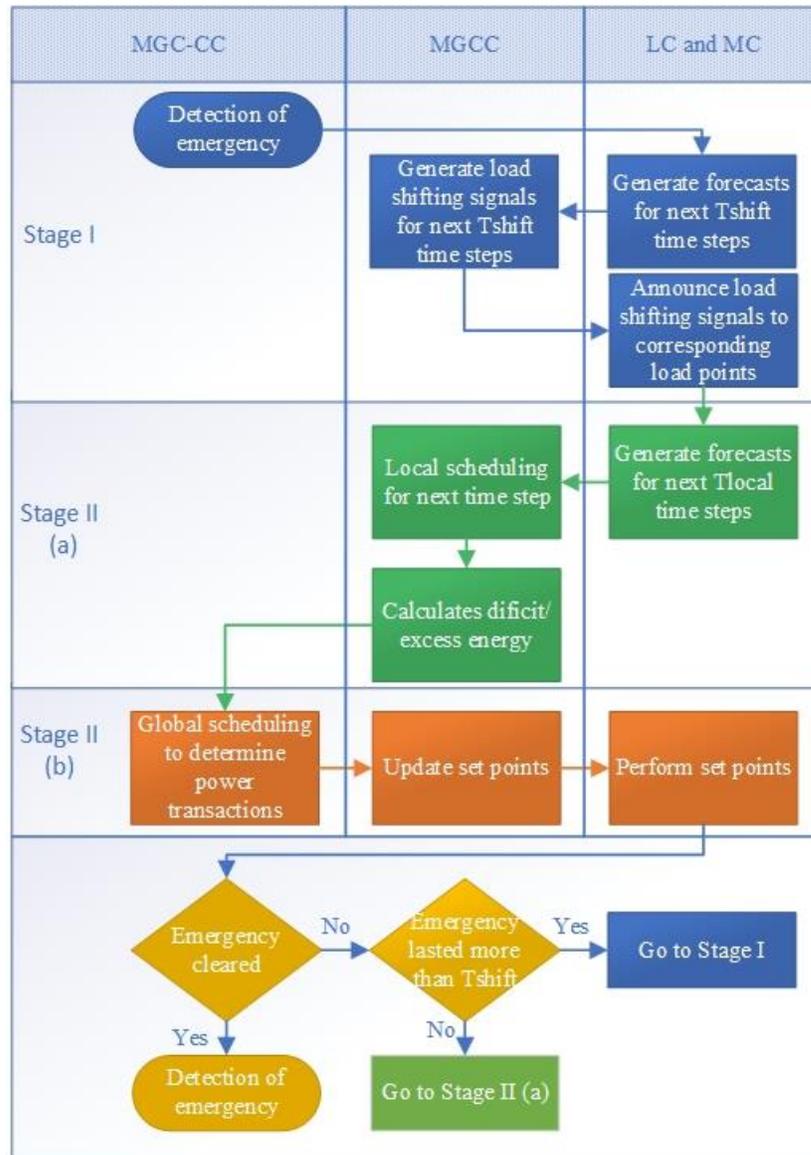

Figure 4.4 Proposed Load Restoration Technique Flow Chart

The next three subsections will cover the mathematical formulation of the following: the preemptive load shifting signals generation, local scheduling and global scheduling

optimization problems. However, although the preemptive load shifting DR program is the first step taken once an emergency is detected, local and global scheduling formulation is presented beforehand for the sake of convenience.

4.3.1 General Optimization of Microgrids Local Scheduling

The RH optimization strategy was adopted at this stage and performed over several time steps, T_{Local}, wherein the cost function of all the periods was minimized. However, it was only the scheduling of the next time step that was applied. The local scheduling optimization problem is expressed as follow:

The objective function:

$$
min \sum_{t=e}^{e+T_{Local}-1} \left\{ \sum_{g=1}^{N_g} C_{g,i}^{CG} \, P_{g,i,t}^{CG} + \sum_{r=1}^{N_r} C_{r,i}^{RG} \, P_{r,i,t}^{RG} + \sum_{l=1}^{N_l} C_{l,i}^{Shed} \, P_{l,i,t}^{Shed} \right.
$$

$$
\left. + \sum_{s=1}^{N_s} C_{s,i}^{Ch} \, P_{s,i,t}^{Ch} + \sum_{s=1}^{N_s} C_{s,i}^{Dch} \, P_{s,i,t}^{Dch} \right\} \Delta t \tag{4.4}
$$

The first and second terms are associated with the cost of generation of DGs. The last two terms are related to the cost of the charging and discharging processes of the ESS units. As the scheduling was performed only during emergencies, the cost of charging of the ESS units was set to a relatively low value or to zero and ensured the maximum utilization of power generation of renewable DGs. Finally, the third term is associated with the cost of loads curtailment. The emergency load shedding DR program was accomplished by setting different load curtailment costs for different priority loads. The determination of a lower curtailment cost associated with lower priority loads facilitated the shedding of lower priority loads when needed, in favor of supplying more critical loads. Furthermore, costs

49

related to the curtailment of loads needed to be relative to the cost of energy generation, to define the operational rules of scheduling. For example, non-critical loads will only be supplied by renewable DGs if their curtailment cost lies between the generation cost of renewable DGs and conventional DGs. The objective function was subject to the following constraints:

Power balance constraints:

$$\sum_{g=1}^{N_g} P_{g,i,t}^{CG} + \sum_{r=1}^{N_r} P_{r,i,t}^{RG} + \sum_{l=1}^{N_l} P_{l,i,t}^{Shed} + \sum_{l=1}^{N_s} P_{s,i,t}^{Dch} = \sum_{l=1}^{N_l} P_{l,i,t}^{Load} + \sum_{l=1}^{N_s} P_{s,i,t}^{Ch} \qquad (4.5)$$

The summation of the power generated by conventional and renewable DGs, the discharged power from ESS units and the amount of curtailed load must all be equivalent to the power demanded by the load points and added to the power charged to the ESS units for every microgrid at each timeslot.

Conventional DGs constraints:

$$I_{g,i,t} X_{g,i,t} P_{g,i}^{CG,min} \leq P_{g,i,t}^{CG} \leq I_{g,i,t} X_{g,i,t} P_{g,i}^{CG,max} \qquad (4.6)$$

$$P_{g,i,t-1}^{CG} - P_{g,i,t}^{CG} \leq DR_{g,i}(1 - d_{g,i,t}) + P_{g,i}^{CG,max} d_{g,i,t} \qquad (4.7)$$

$$P_{g,i,t}^{CG} - P_{g,i,t-1}^{CG} \leq UR_{g,i}(1 - u_{g,i,t}) + P_{g,i}^{CG,max} u_{g,i,t} \qquad (4.8)$$

$$\sum_{t=t}^{t+UT_{g,i}-1} I_{g,i,t} \geq UT_{g,i} u_{g,i,t} \qquad (4.9)$$

$$\sum_{t=t}^{t+DT_{g,i}-1} (1 - I_{i,t}) \geq DT_{g,i} d_{g,i,t} \tag{4.10}$$

$$u_{g,i,t} - d_{g,i,t} = I_{g,i,t} - I_{g,i,t-1} \tag{4.11}$$

$$u_{g,i,t} + d_{g,i,t} = 1 \tag{4.12}$$

The maximum and minimum generation of conventional DGs is determined by equation (4.6). Their boundaries are different from one conventional DG to the next, based on their physical specifications. The generation of a conventional DG is set to zero when it is not committed or unavailable due to a certain failure. The increasing or decreasing amount of a conventional DG generation between two consecutive time steps is restricted by equation (4.7) and (4.8), respectively. The minimum up time and minimum down time constraints of the conventional DG unit are modeled by equations (4.9) and (4.10), respectively. Once the conventional DG is committed, it cannot be turned off until it is up for a certain time, as modeled by equation (4.9). Similarly, once the conventional DG unit is turned off, it cannot be committed again for a period of time. This is ensured by equation (4.10). Equations (4.7-10) depend on the startup and shutdown indicators that are calculated based on the commitment indicators, as shown in equations (4.11) and (4.12).

Renewable DGs constraints:

$$0 \leq P_{r,i,t}^{RG} \leq P_{r,i,t}^{RG,max} \tag{4.13}$$

The utilized power used from by renewable DGs is limited by the amount of the maximum power they can generate at every time step, that which is modeled by equation (4.13).

51

Load shedding constraints:

$$0 \leq P_{l,i,t}^{shed} \leq P_{l,i,t}^{Load} \tag{4.14}$$

The amount of power curtailment of a certain load point cannot exceed the total power demanded at the same load point.

ESSs unit constraints:

$$0 \leq P_{s,i,t}^{Ch} \leq ch_{s,i,t} P_{s,i}^{Ch,max} \tag{4.15}$$

$$0 \leq P_{s,i,t}^{Dch} \leq dch_{s,i,t} P_{s,i}^{Dch,max} \tag{4.16}$$

$$dch_{s,i,t} + ch_{s,i,t} = 1 \tag{4.17}$$

$$SOC_{s,i}^{min} \leq SOC_{s,i,t} \leq SOC_{s,i}^{max} \tag{4.18}$$

$$SOC_{s,i,t+1} = SOC_{s,i,t} + \left(\frac{\left(\eta_{s,i}^{ch} P_{s,i,t}^{Ch} - \frac{P_{s,i,t}^{Dch}}{\eta_{s,i}^{dch}} \right) \Delta t}{C_{s,i}^{ESS}} \right) \tag{4.19}$$

The maximum rate of power charging to the ESS unit is modeled by equation (4.15), while the maximum rate of power discharging from the ESS unit is modeled by equation (4.16). Equation (4.17) was formulated to prevent the charging and discharging of the same ESS unit at the same time. Equation (4.18) identifies the maximum and minimum amount of energy that can be stored in each ESS unit. Finally, equation (4.19) relates the charged or discharged power to the SOC of the ESS unit.

Once local scheduling for the next time step was completed, MGCs in all microgrids, by adjusting their generation set points, calculated the surplus power that local DGs and ESSs

units can participate in during global scheduling. In addition, the amount of local unsupplied demand was also calculated by the MGC. This data was collected and sent to the MGC-CC to determine the power transactions between the microgrids. They are calculated as follows:

Total maximum adjustable power of microgrid's local renewable DGs

$$P_{i,t}^{max-adj,RG} = \sum_{r=1}^{Nr} \left(P_{r,i,t}^{RG,max} - P_{r,i,t}^{RG,I} \right) \tag{4.20}$$

The maximum possible adjustable power of renewable DGs of each microgrid $(P_{i,t}^{max-adj,RG})$ is equal to the summation of the unutilized generation of each renewable DG unit in local scheduling.

Total maximum and minimum adjustable power of microgrid's local conventional DGs

$$E = P_{g,i,t}^{CG,max} - P_{g,i,t}^{CG,i} \tag{4.21}$$

$$F = P_{g,i,t-1}^{CG,ii} + UR_{g,i} - P_{g,i,t}^{CG,i} \tag{4.22}$$

$$P_{g,i,t}^{adj,CG,max} = \begin{cases} \min(E,F), & I_{g,i,t-1}^{ii} = 1 \\ E, & T_{g,i,t}^{off} - DT_{g,i,t} \geq 0 \text{ and } I_{g,i,t-1}^{ii} = 0 \\ 0, & Otherwise \end{cases} \tag{4.23}$$

The maximum adjustable power of each conventional DG unit at each step $(P_{g,i,t}^{adj,CG,max})$ depends on its up-ramp constraint, the commitment state and the scheduled generation in

the previous time step as shown in equations (4.21-23). A and B are constants defined for convenience.

$$P_{g,i,t}^{adj,CG,min} = \begin{cases} 0, & I_{g,i,t}^i = 1 \\ P_{g,i}^{CG,min}, & T_{g,i,t}^{off} - DT_{g,i,t} \geq 0, I_{g,i,t-1}^{ii} = 0 \text{ and } I_{g,i,t}^i = 0 \end{cases} \quad (4.24)$$

The minimum allowable surplus power that a conventional DG unit can participate in to support other microgrids ($P_{g,i,t}^{adj,CG,min}$) depends on the commitment status of the current and previous time step found by local scheduling optimization and global scheduling optimization, respectively as shown in equation (4.24).

To determine the levels of allowable energy participation of conventional DGs in a certain microgrid, a matrix C with a size of $2^{N_g} \times N_g$ is defined. matrix C is defined to invoke all utilization possibilities of the conventional DGs installed in the microgrid. For example, the matrix C for a microgrid with $N_g = 2$ is found to be the following:

$$C = \begin{bmatrix} 1 & 1 \\ 1 & 0 \\ 0 & 1 \\ 0 & 0 \end{bmatrix} = \begin{bmatrix} c_{1,1} & c_{1,2} \\ c_{2,1} & c_{2,2} \\ c_{3,1} & c_{3,2} \\ c_{4,1} & c_{4,2} \end{bmatrix}$$

For N_g conventional DGs, 2^{N_g} allowable surplus energy ranges are calculated to be sent for MGC-CC. The minimum and maximum of each interval are calculated by as follow:

$$\begin{bmatrix} P_{i,1}^{max-adj,CG} & P_{i,1}^{min-adj,CG} \\ P_{i,2}^{max-adj,CG} & P_{i,2}^{min-adj,CG} \\ \vdots & \vdots \\ P_{i,2^{N_g}}^{max-adj,CG} & P_{i,2^{N_g}}^{min-adj,CG} \end{bmatrix} = C \times \begin{bmatrix} P_{1,i,t}^{adj,CG,max} & P_{1,i,t}^{adj,CG,min} \\ P_{2,i,t}^{adj,CG,max} & P_{2,i,t}^{adj,CG,min} \\ \vdots & \vdots \\ P_{N_g,i,t}^{adj,CG,max} & P_{N_g,i,t}^{adj,CG,min} \end{bmatrix} \quad (4.25)$$

The amount of the utilized surplus from conventional DGs of the microgrid based on the global scheduling must have a value that belongs to one these generation ranges.

Total maximum adjustable power of microgrid's local ESS units

$$C = E_{s,i,t+T_{local}} - E_{s,i}^{min} \tag{4.26}$$

$$D = E_{s,i,t} - E_{s,i}^{min} \tag{4.27}$$

$$P_{s,i,t}^{adj,ESS} = \begin{cases} min\left\{ \dfrac{min\left(C, D - \dfrac{P_{s,i,t}^{Dch,i}}{\eta_{s,i}^{dch}}\right) * \eta_{s,i}^{dch}}{\Delta t}, \left(P_{s,i}^{Dch,max} - P_{s,i,t}^{Dch,i}\right) \right\}, & dch_{s,i,t} = 1 \\[4mm] min\left\{ \dfrac{min\left(C, D + P_{s,i,t}^{Ch,i}\eta_{s,i}^{ch}\right) * \eta_{s,i}^{dch}}{\Delta t}, \left(P_{s,i}^{Dch,max} + P_{s,i,t}^{Ch,i}\right) \right\}, & ch_{s,i,t} = 1 \\[4mm] min\left\{ \dfrac{min(C, D) * \eta_{s,i}^{dch}}{\Delta t}, \left(P_{s,i}^{Dch,max}\right) \right\}, & Otherwise \end{cases} \tag{4.28}$$

$$P_{i,t}^{max-adj,ESS} = \sum_{g=1}^{Ng} \left(P_{s,i,t}^{adj,ESS}\right) \tag{4.29}$$

The surplus energy that can be offered by each ESS unit $\left(P_{s,i,t}^{adj,ESS}\right)$ is calculated by equations (4.26-28). It is assumed that every MGC optimizes the charging and discharging processes for the ESSs units for T_{local} time slots, and the stored unused energy at the next $(T_{local} + 1)^{th}$ time slot can be offered by the ESSs units as a surplus power, considering the current SOC and maximum discharging rate. This is completed so that stored energy can work as a backup power source in case a microgrid gets disconnected from the others and has to work autonomously. The total surplus power of a microgrid's local ESSs units

$(P_{i,t}^{max-adj,ESS})$ is calculated by adding the maximum adjustable power of each unit as shown in equation (4.29). Equations (4.26) and (4.27) are presented for convenience.

Total deficit power of microgrids:

$$P_{i,t}^{Deficit} = \sum_{l=1}^{Nl} \left(P_{l,i,t}^{Shed,I} \right) \tag{4.30}$$

The total deficit power of each microgrid $(P_{i,t}^{Deficit})$ is calculated by adding the amount of load curtailment based on each load point in local scheduling.

4.3.2 General Optimization of Microgrids Global Scheduling

Once the data of the surplus or deficit power of each microgrid is received, MGC-CC runs an optimization problem to manage the power transactions between the connected microgrids to help pick up disconnected loads with the least possible cost. The global scheduling optimization problem is expressed in the below equations.

The objective function:

$$min \left\{ \left(\sum_{i=1}^{Ni} C_i^{CG,*} CG_{i,t} + \sum_{i=1}^{Ni} C_i^{RG,*} RG_{i,t} + \sum_{i=1}^{Ni} C_i^{ESS,*} ES_{i,t} + \sum_{i=1}^{Ni} C_i^{Shed*} LS_{i,t} \right. \right.$$
$$\left. \left. + \sum_{i=1}^{Ni} \sum_{j=i+1}^{Ni} C_{i,j}^{Trans} (T_{ij,t}^+ + T_{ij,t}^-) \right) * \Delta t \right\} \tag{4.31}$$

The first two terms represent the total cost of utilization of the surplus power of DGs in each microgrid. The cost associated with the usage of DGs is assumed to be the same as that used in the local optimization problem, excluding the priority that is given to the utilization of DGs of microgrids that offer a larger amount of surplus power compared to those offering less when the cost of generation is the same. The third term is associated

with the cost of utilization of surplus power provided by ESSs units of microgrids. The fourth term represents the cost of load curtailment, meaning the cost of being unable to supply deficit power calculated after the local scheduling optimization. Similarly, if the cost of load curtailment at two load points is the same, the load point with the larger amount of deficit power is given more priority. Finally, the fifth term is associated with the cost of the power transactions between microgrids. The objective function is constrained by the following:

Constraints:

$$CG_{i,t} + RG_{i,t} + ES_{i,t} + LS_{i,t} + \sum_{i=1}^{Ni} \sum_{j \neq i}^{Ni} \left(T_{ij,t}^{+} - T_{ij,t}^{-} \right) = L_{i,t} \qquad (4.32)$$

$$L_{i,t} = P_{i,t}^{Deficit} \qquad (4.33)$$

$$0 \leq RG_{i,t} \leq P_{i,t}^{max-adj,RG} \qquad (4.34)$$

$$\sum_{n=1}^{2^{Ng}} (P_{i,n}^{min-adj,CG} Z_n) \leq CG_{i,t} \leq \sum_{n=1}^{2^{Ng}} (P_{i,n}^{max-adj,CG} Z_n) \qquad (4.35)$$

$$\sum_{n=1}^{2^{Ng}} Z_n = 1 \qquad (4.36)$$

$$0 \leq ES_{i,t} \leq P_{i,t}^{max-adj,ESS} \qquad (4.37)$$

$$0 \leq T_{ij,t}^{+} \leq \tau_{ij} T_{ij}^{max} \quad i \neq j \qquad (4.38)$$

$$0 \leq T_{ij,t}^{-} \leq \tau_{ij} T_{ij}^{max} \quad i \neq j \qquad (4.39)$$

$$0 \leq LS_{i,t} \leq L_{i,t} \qquad (4.44)$$

All the above constraints are applied for each different microgrid i. The balance of supply and demand in each microgrid is guaranteed using Equation (4.32). The utilized surplus

power of conventional DGs, renewable DGs and ESSs units, with the added net income power from other microgrids, must equal the load that needs to be supplied. In the global optimization problem, $(L_{i,t})$ equals the deficit power found after local scheduling as shown in equation (4.33). Equation (4.34) is formulated to ensure that the utilized energy from the renewable DGs of the microgrid does not exceed its maximum surplus power. Equations (3.35) and (3.36) ensure that the utilized surplus power from the microgrid is within one of the possible power ranges. Equation (4.37) was formulated to set the boundaries for the use of the surplus power from ESS of the microgrid. The power transferred from and to the microgrid should not exceed the maximum capacity of the tie lines. This is expressed by equations (3.38) and (3.39). Finally, equation (4.40) was modeled so that load shedding of the global scheduling does not exceed the deficit power of the local scheduling.

By solving the optimization problem, the amount of utilized power of the surplus power – offered by different resources – is determined and sent to the MGCs of the microgrids. After receiving this information, the MGCs then update the operational schedule, while considering the cost and technical constraints of the different units at each microgrid.

4.3.3 Generation of preemptive load shifting signals

The preemptive load shifting DR program is applied as the first step of the proposed load restoration technique. The main objective is to reshape the load profile in accordance with the availability of power resources, mainly renewable DGs, and to support the restoration of high priority loads. This is completed by formulating an optimization problem like that of the local scheduling problem except that some loads can shift from one time step to another. The optimization problem covers T_{shift} time steps. T_{shift} should be set to a

suitable value that is convenient for the participating customers and shouldn't exceed the

expected duration of emergency T_{emrg}. The load shifting signals generation optimization

problem is expressed as follows:

Objective function:

$$
\begin{aligned}
min \sum_{t=e}^{e+T_{shift}-1} & \left\{ \left(\sum_{g=1}^{N_g} C_{g,i}^{CG} P_{g,i,t}^{CG} + \sum_{r=1}^{N_r} C_{r,i}^{RG} P_{r,i,t}^{RG} + \sum_{l=1}^{N_l} C_{l,i}^{Shed} P_{l,i,t}^{Shed} \right. \right. \\
& \left. + \sum_{s=1}^{N_s} C_{s,i}^{Ch} P_{s,i,t}^{Ch} + \sum_{s=1}^{N_s} C_{s,i}^{Dch} P_{s,i,t}^{Dch} \right) \Delta t \right\} \\
& + \sum_{t=e}^{e+T_{emrg}-1} \sum_{t'=e,t'\neq t}^{e+T_{shift}-1} C_{t,t'}^{shift} P_{t,t'}^{Shift} \Delta t
\end{aligned}
\tag{4.41}
$$

The objective function is similar to the one used in the formulation of the local scheduling

optimization problem where a sixth term is added to represent the cost of load shifting from

one time to another. The cost associated with load shifting is small when the shifting of the

load is permitted and set high when the shifting is not permitted. The objective function is

subjected to the following:

Constraints:

$$
\begin{aligned}
\sum_{t'=e,t'\neq t}^{e+T_{emrg}-1} P_{i,(t',t)}^{shift} & + \sum_{g=1}^{N_g} P_{g,i,t}^{CG} + \sum_{r=1}^{N_r} P_{r,i,t}^{RG} + \sum_{l=1}^{N_l} P_{l,i,t}^{Shed} \\
& + \sum_{l=1}^{N_s} P_{s,i,t}^{Dch} = \sum_{l=1}^{N_l} P_{l,i,t}^{Load} + \sum_{l=1}^{N_s} P_{s,i,t}^{Ch} \\
& + \sum_{t'=e,t'\neq t}^{e+T_{emrg}-1} P_{i,(t,t')}^{shift}
\end{aligned}
\tag{4.42}
$$

$$\sum_{t'=e,t'\neq t}^{k+T_{emrg}-1} P_{i,(t,t')}^{shift} \leq IF_{i,t} \tag{4.43}$$

$$\sum_{t'=e,t'\neq t}^{k+T_{emrg}-1} P_{i,(t',t)}^{shift} \leq OF_{i,t} \tag{4.44}$$

Equation (4.42) is built to sustain the power balance in each microgrid for every time step. Power balance constraint is similar to the one in the local scheduling optimization problem, aside from two added terms. Load shifting from the current time step to other time steps is considered a source of generation, while the shifted demand from other time steps to the current time step is considered an added load. Equation (4.43) and (4.44) restrict the amount of shifted load to or from each time step, respectively. $OF_{i,t}$ in equation (4.44) is the amount of shiftable loads of time step t. Finally, conventional DGs, renewable DGs, load shedding, and ESS unit constraints defined in subsection (4.3.1) and expressed in equations (4.6-18) are also constraints in this optimization problem.

4.4   Load Restoration Technique - Success Index (SI)

To evaluate the performance of the proposed load restoration technique, a success index (SI) was created in this section. The load restoration technique performance is assessed relative to the performance of load restoration of microgrids working autonomously in islanded mode (non-cooperative operation). The success index is calculated by dividing the scaled amount of restored load of the total load in all microgrids through the implementation of the restoration technique and by the scaled amount of the restored load when the microgrids worked autonomously as shown in equation (4.46).

$$SI = \frac{\sum_{i=1}^{Ni} \sum_{t=e}^{e+T_{DE}-1} \sum_{l=1}^{Nl} S_{i,l} * (P_{l,i,t}^{Load} - LS_{i,l,t}) \Delta t}{\sum_{i=1}^{Ni} \sum_{t=e}^{e+T_{DE}-1} \sum_{l=1}^{Nl} S_{i,l} * (P_{l,i,t}^{Load} - P_{l,i,t}^{Shed}) \Delta t} \qquad (4.45)$$

Where T_{DE} is the actual duration of emergency and S is a scaling factor that depends on the priority of the load points as shown in Table 4.1.

Table 4.1 Load Restoration Technique Success Index Scaling Factor

Load Restoration Technique Scaling Factor		
$S_{l,i}^{HP}$	$S_{l,i}^{MP}$	$S_{l,i}^{LP}$
1.2	1	0.8

Larger restoration technique success index values indicated better performance of the proposed restoration technique in which a lower amount of load curtailment was happening. In addition, values higher than 1 reflected an enhancement of the overall system performance, while value below 1 indicated that the microgrid autonomous operation gave better results than the microgrid cooperative operation.

CHAPTER 5

TEST SYSTEM AND SIMULATIONS

In this chapter, the input data needed for studying the proposed technique through simulations are presented. The demand profile, the forecasted wind, and solar generation used are presented. Additionally, the parameters for modeling the components of the test system are stated. Furthermore, the performance of the proposed restoration technique will be studied through the simulation of different outage scenarios, and a sensitivity analysis will be performed. Finally, discussion and analysis of the results will be provided.

5.1   Input Data and Test System

In this section, the distribution system consists of three microgrids as shown in Figure 5.1. This is considered the test system. In normal conditions, the distribution system presumes a radial energy delivery configuration. In this configuration, the demand of microgrids is supplied by the utility grid and local resources only.
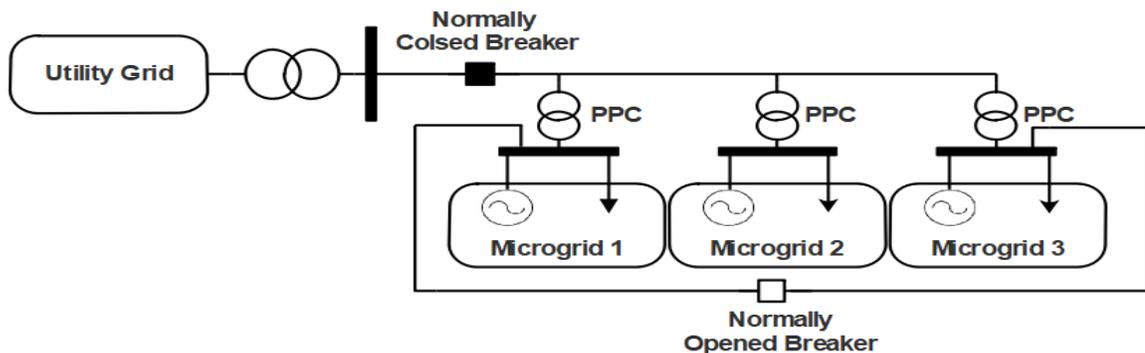

Figure 5.1 Test System

Once a contingency on the utility grid side is detected, the distribution system disconnects itself through the normally-closed circuit breaker. The microgrids are then networked using the normally-opened circuit breaker to facilitate energy transaction between them. Microgrids can be classified into residential and commercial microgrids based on the type of customer consumption. To represent the residential load in the model, data from residential load consumption in Dammam, Saudi Arabia was considered. Figure 5.2 shows the normalized daily average for residential power consumption in the month of July in 2015. As seen in the figure, the daily peak consumption occurred at 3:00 PM, and the daily minimum consumption occurred at 6:00 AM. For commercial microgrids, typical daily commercial load data was used to simulate the demand as shown in Figure 5.3.
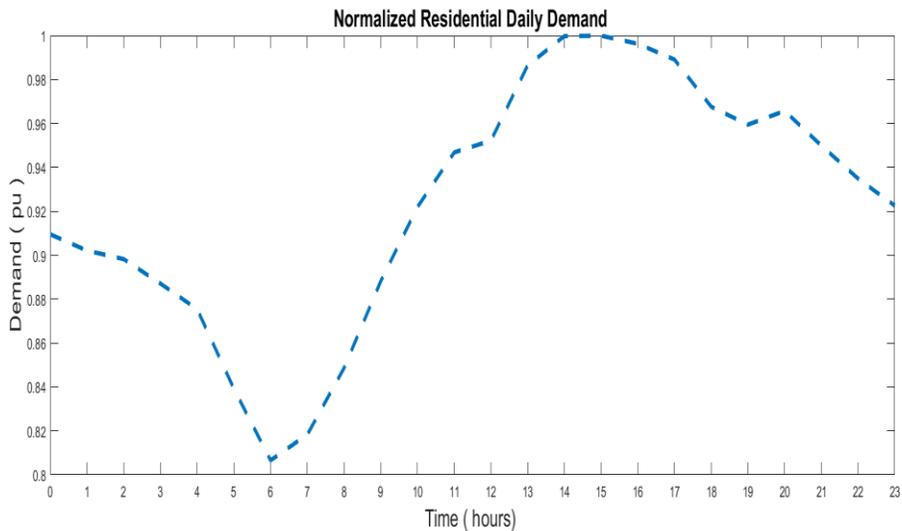

Figure 5.2 Normalized Average Daily Residential Consumption in Dammam for The Month of July 2015
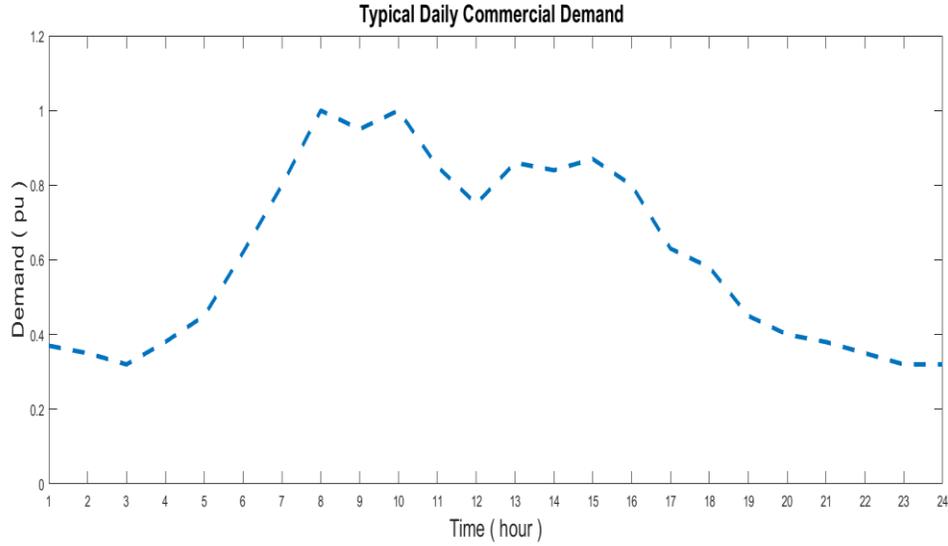
Figure 5.3 Normalized Typical Daily Commercial Demand

The load points in each microgrid are categorized into low, medium, and high priority. It is assumed that each type of load point posits a certain percentage of the total hourly demand, summarized in Table 5.1.

Table 5.1 Load Points Types Percentage of The Hourly Total Demand

Percentage of each loads types of the hourly total demand		
Low priority load points	Medium priority load points	High priority load points
5%	60%	35%

To find the output generation, solar irradiance and ambient temperature data – measured by the Research Institute (RI) at KFUPM in the Eastern Province of Saudi Arabia in 2016 – are used as an input to the solar PV generator operational model discussed in section (3.1.1). Figure 5.4 depicts the average daily solar irradiance for the month of July in 2016. The specifications of the solar PV modules used to build the PV generator system is shown in Table 5.2 [89]. It is also assumed that an efficient maximum point tracker is installed in the PV system and that all PV modules are subject to the same surrounding conditions.

64
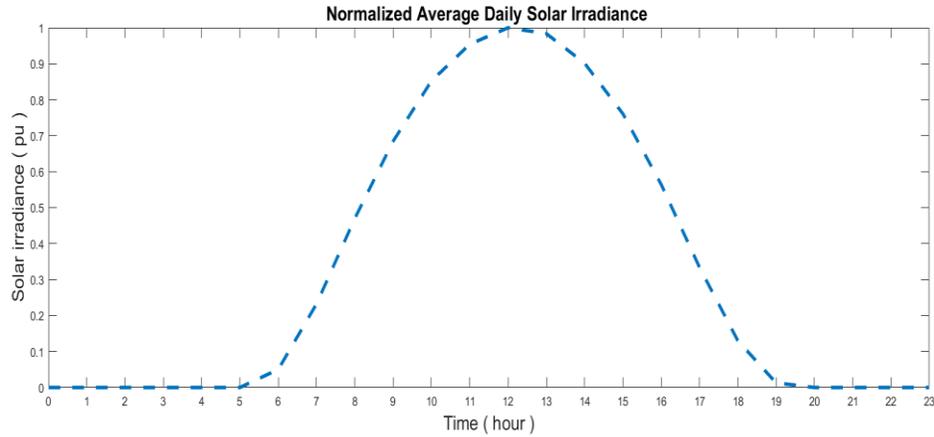
Figure 5.4 Normalized Average Daily Solar Irradiance in Dhahran for The Month of July 2016

Table 5.2 Technical Specifications of Used PV Modules

Specification of PV Module	
Manufacturer	MITSUBISHI ELECTRIC
Model name	PV-MLU255HC
Cell type	Mono-crystalline silicon
Maximum power rating (P_{Max})	255 [Wp]
Open circuit voltage (V_{OC})	37.8 [V]
Short circuit current (I_{SC})	8.89 [A]
Maximum power voltage (V_{MPP})	31.2 [V]
Maximum power current (I_{MPP})	8.18 [A]
Normal operating cell temperature (N_{OT})	45.7 [℃]
Temp. Coeff. of Isc (K_I)	+0.056 [%/°C]
Temp. Coeff. of V_{OC} (K_v)	-0.350 [%/°C]

The input of the operational model of a wind generator, i.e. the wind speed, is calculated using the shape and scale factors of the Weibull distribution function. Shape and scale factors were found using historical data recorded over 20 years and measured in Dhahran [90]. Table 5.3 shows the monthly scale and shape factors as per these records.

Once the forecasting the wind speed is determined, it is scaled to the height of the hub of the wind turbine as discussed in section (3.1.2). At this height, a typical value of (1/7),

corresponding to low roughness sites, is chosen as a value of the power law exponent (α) [91].

Table 5.3 Monthly Shape and Scale Factor of Wind Speed in Dhahran

Monthly Shape and Scale Factor					
Month	σ	c	Month	σ	c
Jan	2.40	4.77	Jul	2.50	5.54
Feb	2.45	4.85	Aug	2.30	4.91
Mar	2.55	5.15	Sep	2.20	4.18
Apr	2.40	5.06	Oct	2.05	4.09
May	2.40	5.52	Nov	2.20	4.38
Jun	2.60	6.51	Dec	2.00	4.68

The wind speed for the month of July was generated using the corresponding shape and scale factors of the Weibull function, and the normalized average daily wind speed is shown in Figure 5.5.
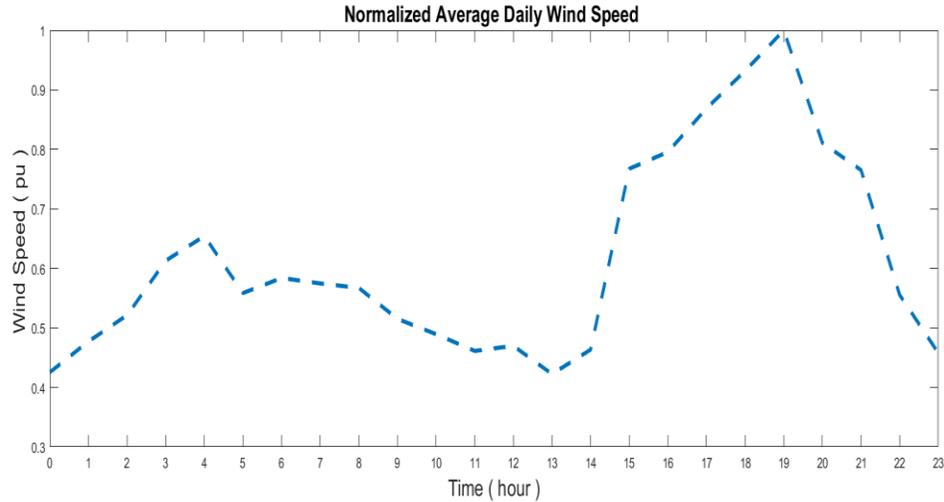

Figure 5.5 Normalized Average Daily Wind Speed in Dhahran for The Month of July

In this study, a 3.5 kW wind turbine, manufactured by raum ENERGY and whose specifications and practical power curve are listed in Table 5.4 and Table 5.5, respectively

[92], was used. The power curve was provided by the manufacturer and states the measured output power corresponding to certain wind speeds.

Table 5.4 Wind Turbine Technical Specifications

Wind Turbine System Specifications	
Rated power (P_r)	3.5 [kW]
Cut-in speed (V_{cin})	2.8 [m/s]
Cut-out speed (V_{co})	22 [m/s]
Rated speed (V_r)	11 [m/s]
Hight of turbine's hub (h)	14.5 [m]

Table 5.5 Wind Turbine Practical Power Curve

Wind Turbine Practical Power Curve			
Wind Speed [m/sec]	Power Out [W]	Wind Speed [m/sec]	Power Out [W]
3	51	8	1569
4	134	9	2233
5	297	10	3064
6	563	11	3500
7	1000	12	3500

As discussed in section (3.1.2) the generation characteristics of the wind turbine are fit in cubic spline interpolation. For the break points of wind speed and output power provided by the manufacturer, nine third order polynomials for power curve fitting was formulated. The coefficients of the cubic spline polynomials are summarized in Table 5.6 and the resultant power curve is shown in Figure 5.6.
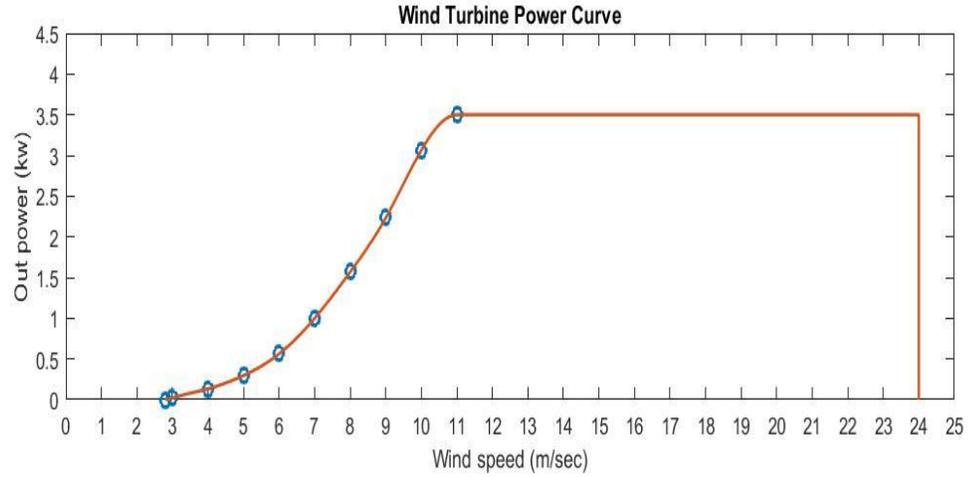
Figure 5.6 Fitted Wind Turbine Output Power Curve

Table 5.6 Coefficient of Cubic Spline Polynomials

	Coefficients of Cubic Spline Polynomials				
n	a_n	b_n	c_n	d_n	Speed Bounds
1	-4354.5	2145.9	0	0	$V \in (2.8,3]$
2	214	-466.82	335.82	51	$V \in (3,4]$
3	-56.369	175.19	44.184	134	$V \in (4,5]$
4	34.474	6.0787	22.45	297	$V \in (5,6]$
5	-13.526	109.5	341.03	563	$V \in (6,7]$
6	-19.369	68.921	519.45	1000	$V \in (7,8]$
7	54.001	10.815	599.18	1569	$V \in (8,9]$
8	-124.64	172.82	782.82	2233	$V \in (9,10]$
9	-117.45	-201.09	754.55	3064	$V \in [10,11]$

It is assumed that all microgrids have the same annual peak demand of 350 kW for both types of microgrids, namely, commercial and residential microgrids. The specifications of

the installed ESSs and conventional DGs in the MMG test distribution system are listed in Table 5.7 and Table 5.8, respectively.

Table 5.7 Specifications of The Installed ESSs

Technical specifications of ESSs units							
Unit s	Microgrid i	$C_{s,i}^{ESS}$ $[kWh]$	$P_{g,i}^{Ch/Dch,max}$ $[kW]$	$\eta^{ch}_{s,i}$	$\eta^{dch}_{s,i}$	$SOC^{min}_{s,i}$	$SOC^{max}_{s,i}$
1	1	520	26	0.95	0.95	20%	90%
2	2	650	32.5	0.95	0.92	20%	90%
3	3	780	40	0.97	0.95	20%	90%

Table 5.8 Specifications of The Installed Conventional DGs

Technical specifications of conventional DG units							
Unit g	Microgrid i	$P_{g,i}^{CG,max}$ $[kW]$	$P_{g,i}^{CG,min}$ $[kW]$	$UT_{g,i}$ $[hour]$	$DT_{g,i}$ $[hour]$	$UR_{g,i}$ $[kW]$	$DR_{g,i}$ $[kW]$
1	1	350	28	1	2	50	50
2	2	150	25	1	1	50	50
3	3	70	7	1	1	40	40

All the ESSs units are assumed to be 70 % charged initially. The maximum per unit total generation of the renewable DGs in respect to the annual peak demand in microgrid 1, 2 and 3 are equal to 0.1 pu, 0.8 pu and 1 pu, respectively. The distribution of the capacity of renewable based generation among PV and Wind generation systems in each microgrid is shown in Table 5.9.

Table 5.9 Maximum Generation Capacity of Renewable DGs in Microgrids

Maximum generation capacity of PV generation and wind generation systems in each microgrid			
Unit r	Type	Microgrid i	Maximum capacity $P_{r,i}^{RG,max}$, $[kW]$
1	PV generation System	1	20
2	Wind generation system		15
3	PV generation System	2	200
4	Wind generation system		80
5	PV generation System	3	50
6	Wind generation system		300

The costs associated with the local and global scheduling optimization problems are assumed to be the same. However, as mentioned earlier, resources of microgrids that offer larger amount of surplus power are given priority if the cost offered by the microgrids used for surplus power is the same. The costs associated with DGs generation, ESSs charging and discharging, load shifting and shedding and power transactions between microgrids are shown in per unit of cost for generation of conventional DGs as listed in Table 5.10.

Table 5.10 Costs Used in Local and Global Optimization

Costs associated with local and global optimization problems									
C^{CG}	C^{PV}	C^{Wind}	C^{Ch}	C^{Dch}	$C^{Shed,LP}$	$C^{Shed,MP}$	$C^{Shed,HP}$	C^{Shift}	C^{Trans}
1	0.32	0.48	0	0.8	5	10	15	0	1.4

It is always preferable for microgrids to be conservative, therefore the cost of charging ESSs is set to zero to help conserve excess energy in the case of an emergency. The aim of preemptive load shifting is not to reduce the peak demand but rather to reschedule the demand shape in accordance with the availability of the sources, hence, load shifting is allowed between any two-time slots by setting associated costs to zero. The rules of

70

microgrid operation can be decided and controlled by tuning the costs. For example, conventional DGs will not be dispatched to supply low priority loads if the curtailment cost is lower than the generation cost. The costs of load shedding are set to ensure that they will be supplied if possible, but lower priority load points will be first to shed in favor of higher priority load points.

5.2   Simulations

In the following section, three outage scenarios are simulated. In the first scenario, the MMG distribution system is composed of three residential microgrids. A contingency is expected to occur on the utility side which will cause the MMG distribution system to operate in the islanded mode for 8 consecutive hours. In addition, the local scheduling horizon (T_{local}) of the microgrids is set to 3 hours and the tie-lines capacity connecting them is set to 50 kW. The second outage scenario is identical to the first outage scenario except that Microgrid-1 assumes a commercial load profile. Finally, the third outage scenario is identical to the first scenario, but to simulate more severe emergencies, the conventional DG installed in Microgrid-1 is assumed to be unavailable in the last two hours of the emergency. In addition, Microgrid-2 is assumed to be isolated from the other microgrids at the beginning of the emergency for two hours. Table 5.12 summarizes the operating parameters and outage conditions of the three scenarios.

In each scenario, 24 outages spanning 8 hours with different starting times will be simulated. To evaluate the performance, the following three steps will be completed within the simulation of each outage scenario. Firstly, microgrids will be created to operate

71

independently from one another with no power transactions between them. The unsupplied energy during each outage will then be calculated. Secondly, the proposed restoration technique will be applied to the MGG and the unsupplied energy during each outage will be calculated again. Finally, the restoration technique SI will be calculated for each outage based on the previous two steps.

Table 5.11 Simulated Outage Scenarios Summary

Simulated Outage Scenarios Summary			
Outage parameters	Scenario I	Scenario II	Scenario III
Types of microgrids	residential	2 residential 1 commercial	3 residential
Outage duration	8 hours	8 hours	8 hours
Local scheduling horizon	3 hours	3 hours	3 hours
Allowable percentage of load shifting	5%	5%	5%
Tie line capacity	50 kW	50 kW	50 kW
Additional outage condition	-	-	1-Microgrid-2 is isolated for first two hours of the outage. 2-Microgrid-1's conventional DG unavailable in last two hours of the outage

5.2.1 Scenario I (Three Residential Microgrids)

The MMG distribution system was disconnected from the main utility supply for 8 consecutive hours. The starting time of the emergency varied to cover 24 hours of the day,

and the local scheduling horizon T_{local} was set to 3 hours. All the microgrids were assumed to be of the residential type and the networking tie lines had a capacity of 50 kW each.

In the beginning, each of the microgrids was made to operate independent of the other and was disconnected from the main utility grid. The total curtailed energy for the three microgrids during the duration of the emergency for different emergency starting times is presented in Figure 5.7. Each bar in Figure 5.7 represents the MGG distribution system unsupplied energy during an outage that lasted 8 hours and started at a certain time specified on the x-axis.
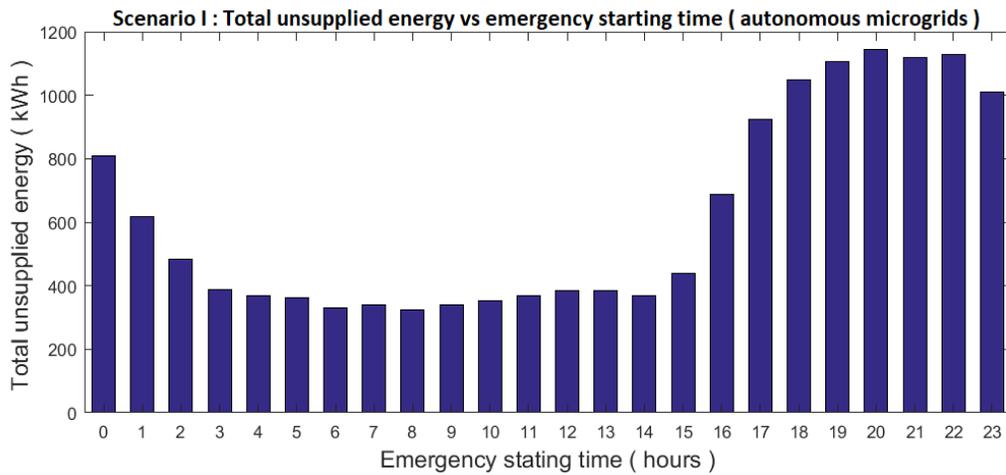

Figure 5.7 Scenario I: Total Unsupplied Energy vs Emergency Starting Time (autonomous microgrids)

Next, the load restoration technique was applied and the microgrids were made to cooperate with each other. The resulting total unsupplied energy for different emergency starting times is shown in Figure 5.8.
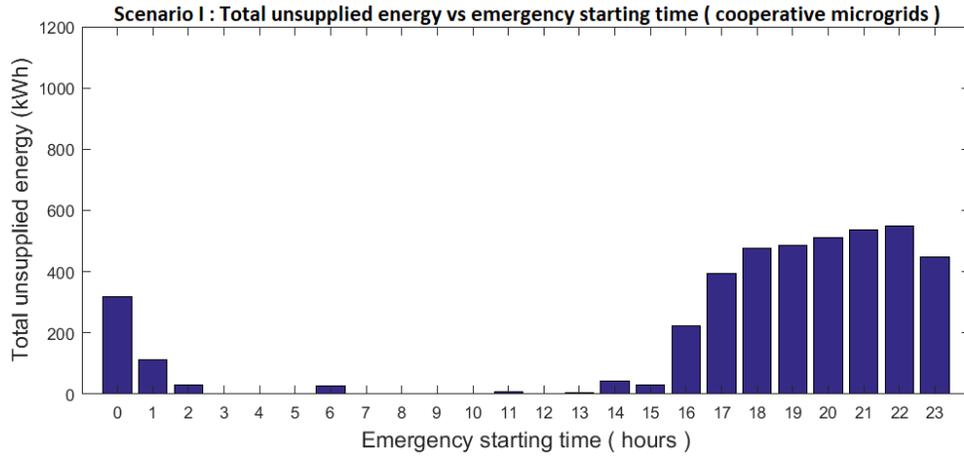
Figure 5.8 Scenario I: Total Unsupplied Energy vs Emergency Starting Time (cooperative microgrids)

The total amount of energy curtailment for all starting times of emergency decreased, especially when the starting time of the emergency was during the day. This was expected as Microgrid-1 was able to supply its load because it had a capacity of dispatchable generation that covered its demand. Consequently, Microgrid-1 had the flexibility to support other microgrids. In addition, Microgrid-2 had a relatively high capacity for the solar generation system which peaks at the day hours and can share surplus energy during these periods. The total energy transactions from microgrid-1, 2 and 3 for different emergency starting times are shown in Figure 5.9, Figure 5.10 and Figure 5.11, respectively.
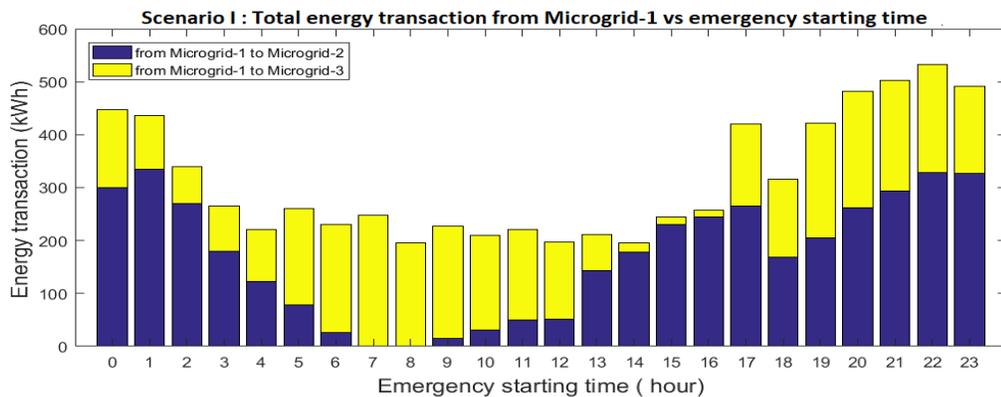

Figure 5.9 Total Energy Transaction from Microgrid-1 vs Emergency Starting Time
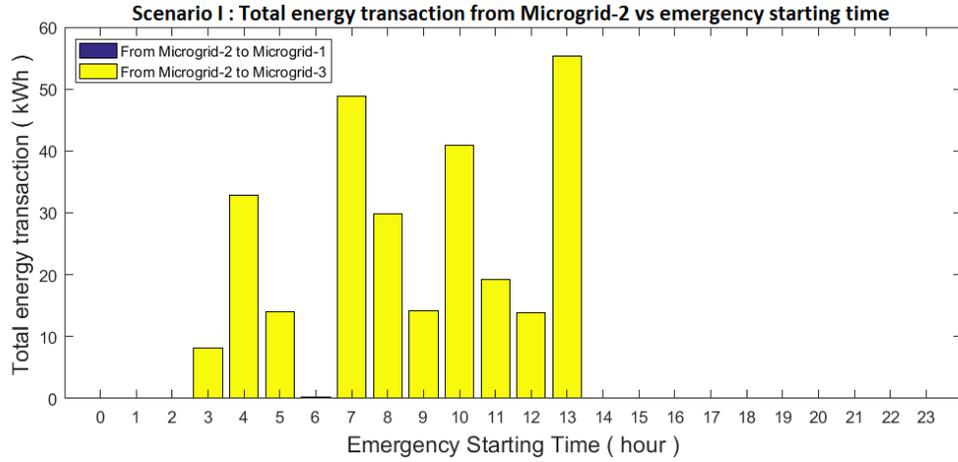
Figure 5.10 Scenario I: Total Energy Transaction from Microgrid-2 vs Emergency Starting Time
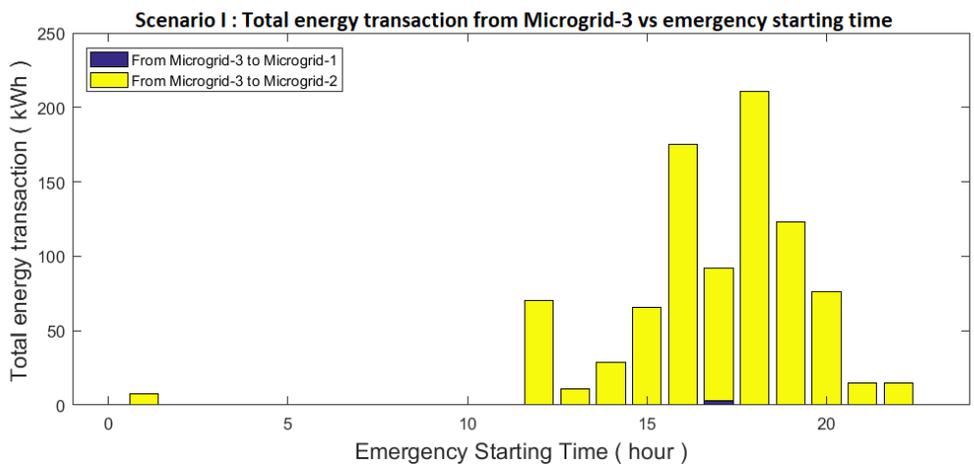

Figure 5.11 Scenario I: Total Energy Transaction from Microgrid-3 vs Emergency Starting Time

Energy transaction from Microgrid-1 to Microgrid-2 dropped when the emergency occurred during day time due to the relatively high capacity for the solar generation system in Microgrid-2. As it was observed, the energy transaction from Microgrid-2 was almost zero during nighttime-emergencies while the transaction from Microgrid-3 was nearly zero during daytime-emergencies. This was because the capacity of the PV generation system was high in Microgrid-2, while the capacity of the wind generation system was high in Microgrid-3. With regards to Microgrid-1, the power transacted to it from Microgrid-2 and Microgrid-3 equaled zero for almost all emergency starting times. Despite the capacity of

75

dispatchable generation that covered the demand in Microgrid-1, there was a need for support from other microgrids as seen in Figure 5.10 and Figure 5.11. This may be due to the power output up ramp constraint of the installed conventional DG.

Finally, SI was calculated for all different emergency starting times as shown in Figure 5.12, and the average was found to be around 1.0567. The proposed restoration technique showed its ability to enhance the overall system performance compared to when microgrids are made to operate autonomously. This was indicated by the SI value larger than one. Finally, it can be concluded that the overall performance of load restoration was improved by more than 50% when applying the proposed technique.
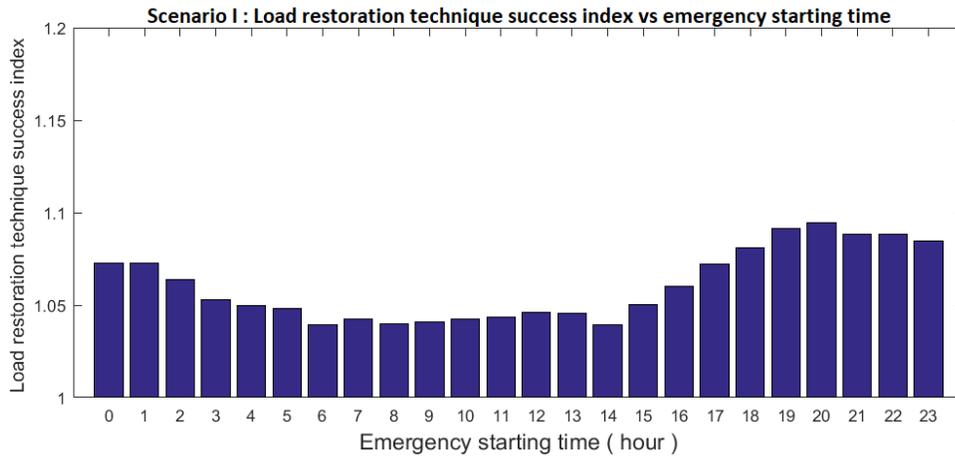

Figure 5.12 Scenario I: Load Restoration Technique Success index vs Emergency Starting Time

5.2.2 Scenario II (Two Residential and One Industrial Microgrids)

Like outage Scenario I, the MMG distribution system was disconnected from the main utility supply for 8 consecutive hours with a local scheduling horizon of 3 hours in Scenario II. In addition, the capacity of the networking tie lines was the same (50 kW) and all steps completed in Scenario I were completed in Scenario II. However, unlike Scenario I, Microgrid-1 posited a commercial load.

76

As in Scenario I, each microgrid was made to operate as an autonomous entity and the total amount of curtailed load for different emergency starting times was calculated as shown in Figure 5.13.
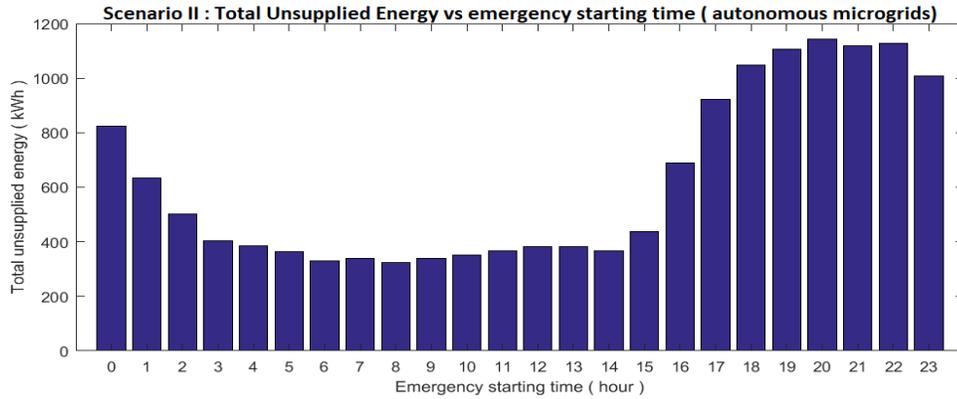

Figure 5.13 Scenario II: Total Unsupplied Energy vs Emergency Starting Time (autonomous microgrids)

By means of deduction, the resultant curves in both Scenario I and Scenario II are almost identical. When the load type in Microgrid-1 was changed to commercial, the microgrid was still be able to cover the load due to the instillation of conventional DG. However, the change was more evident when the microgrids were made to cooperate with each other. The total curtailed energy for different emergency starting times after applying the proposed restoration technique is shown in Figure 5.14.
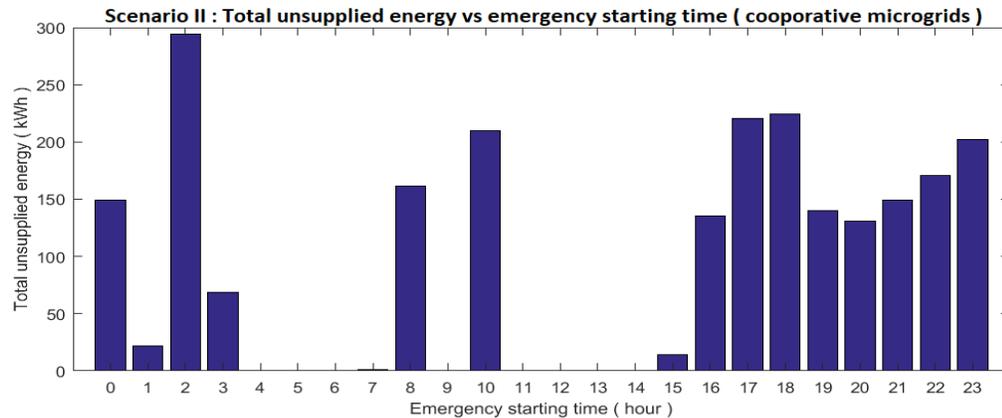

Figure 5.14 Total Unsupplied Energy vs Emergency Starting Time (cooperative microgrids)

77

Compared to Scenario I, the overall load curtailment decreased. This as expected since the demand for commercial customers was high only during the working hours of the day, which gave Microgrid-1 more flexibility in supporting other microgrids. However, load curtailment caused by emergencies during the morning was higher than it was in Scenario I because the load at Microgrid-1 was at its peak during these times.

The total energy transactions from microgrid-1, 2 and 3 for different emergency starting times are shown in Figure 5.15, Figure 5.16 and Figure 5.17, respectively.
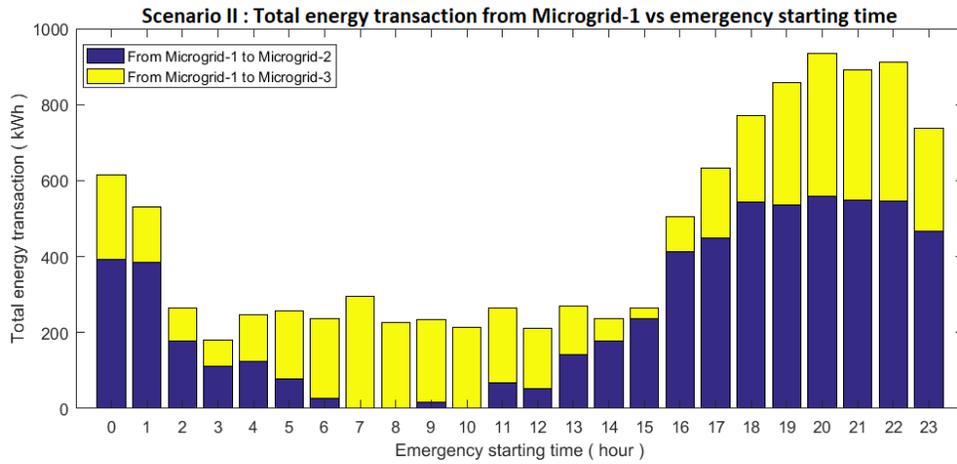

**Figure 5.15 Scenario II: Total Energy Transaction from Microgrid-1 vs Emergency Starting Time**
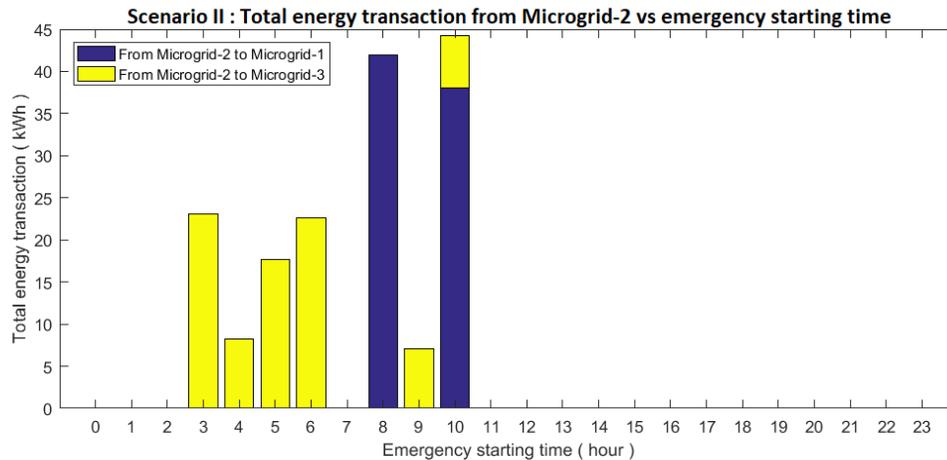
Figure 5.16 Scenario II: Total Energy Transaction from Microgrid-2 vs Emergency Starting Time
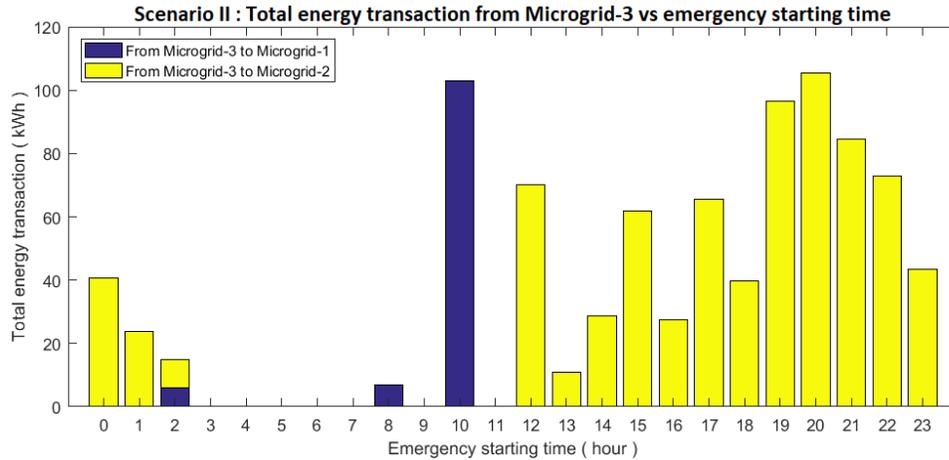
Figure 5.17 Scenario II: Total Energy Transaction from Microgrid-3 vs Emergency Starting Time

The same holds true for the power transaction of Microgrid-2 and 3. Most of the power transaction from Microgrid-2 happened during the daytime, while power transaction from Microgrid-3 was concentrated in nighttime. The energy transaction From Microgrid-1 increased compared to Scenario I, especially during emergencies occurring during nighttime. The main reason for this increase was that commercial demand was low during non-working hours in the day. However, compared to Scenario I, energy transactions to Microgrid-1 also increased, especially during daytime emergencies. This happened because of the up-ramp constraint imposed on the output generation of conventional DG installed in Microgrid-1. Commercial demand steeply increased between non-working hours and working hours in which the rate of increase in generation of conventional DG might not have been able to catch this change.

The load restoration technique SI was calculated for all possible emergency starting times as shown in Figure 5.18. The overall performance of the system was enhanced by the application of the proposed restoration technique where the average restoration SI was calculated to be 1.0819. Restoration success index was at its highest for nighttime-

emergencies occurring where Microgrid-1 had a low demand, therefore, it was capable of supplying deficit energy in Microgrid-2 and 3, and the maximum was found to be 1.1824.
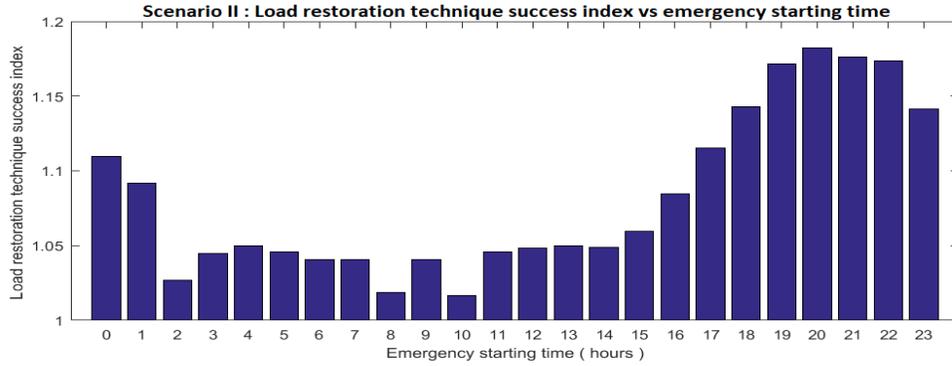
Figure 5.18 Scenario II: Load Restoration Technique Success Index vs Emergency Starting Time

5.2.3 Scenario III (Three Residential Microgrids –Severe Conditions)

Scenario III was identical to Scenario I but to simulate more severe emergencies, the conventional DG installed in Microgrid-1 was not available to be dispatched in the seventh and eighth hour of the emergency duration. In addition, Microgrid-2 was isolated from the other microgrids at the beginning of the emergency for two hours.

Based on these assumptions, microgrids are made to supply only their local loads and operate autonomously. The total load curtailment for all possible starting times of the emergency is plotted in Figure 5.19.
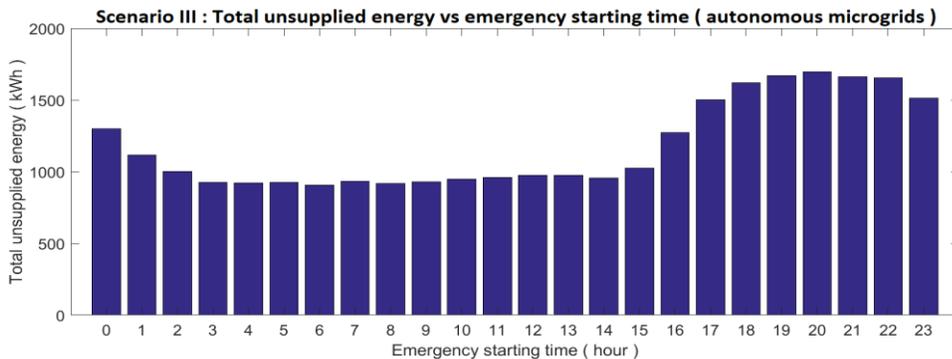
Figure 5.19 Scenario III: Total Unsupplied Energy vs Emergency Starting Time (autonomous microgrids)

80

Compared to Scenario I, the amount of unsupplied energy increased dramatically for all possible starting times of emergencies. This increase was because Microgrid-1 mainly depended on the installed conventional DG, which was assumed to be out of service for two hours during the emergency.

For the sake of comparison, the total unsupplied energy for emergencies with all possible starting times after applying the proposed restoration technique was calculated as shown in Figure 5.20.
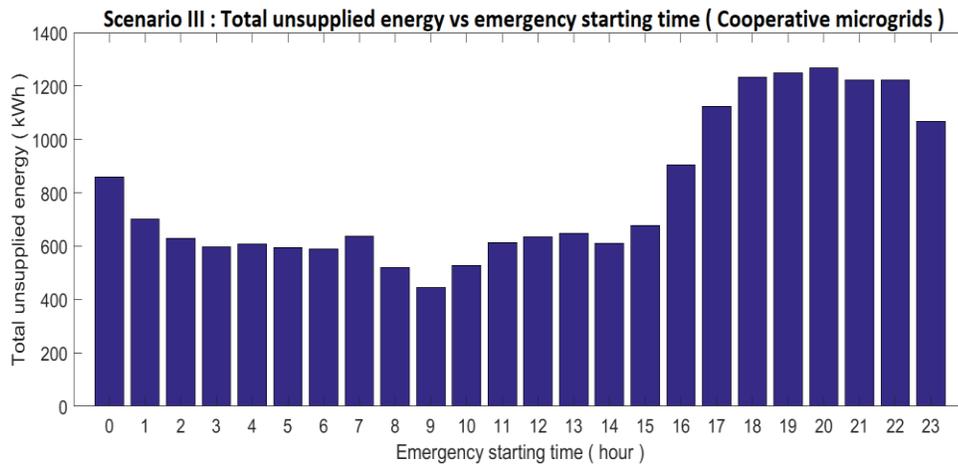
Figure 5.20 Scenario III: Total Unsupplied Energy vs Emergency Starting Time (cooperative microgrids)

Compared to the microgrids cooperative operation completed in Scenario I, the total unsupplied energy for almost all emergency starting times increased. This increase is reasonable as the MMG distribution system was subjected to more severe conditions. It can be deduced from the figure that the increase in unsupplied energy was strongly evident for emergencies that occurred during the day. This was due to the disconnection of Microgrid-3 from the other microgrids. Microgrid-3, normally, depends on the energy transactions from Microgrid-1 and 2 during daytime emergencies because of its low local

generation. This dependency was restricted in Scenario III, which caused this increase in the unsupplied energy.

The total energy transactions from Microgrid-1, 2 and 3 for different emergencies for different durations is shown in Figure 5.21, Figure 5.22 and Figure 5.23, respectively.
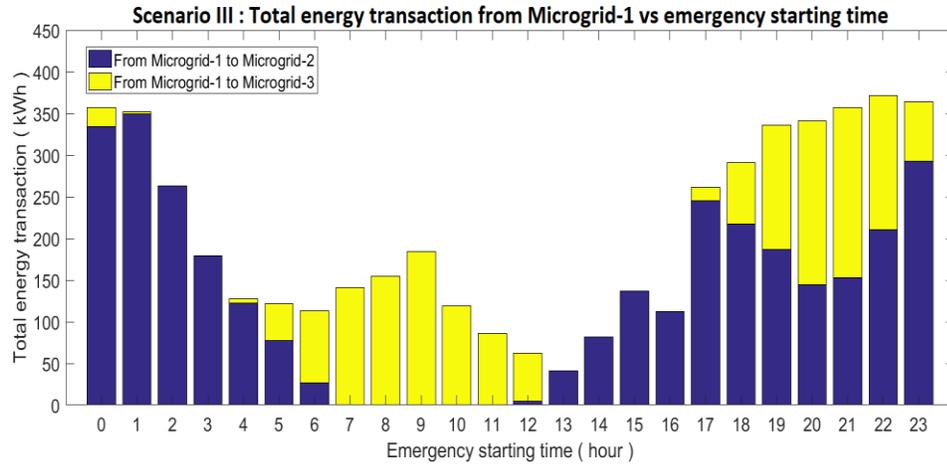
Figure 5.21 Scenario III: Total Energy Transaction from Microgrid-1 vs Emergency Starting Time
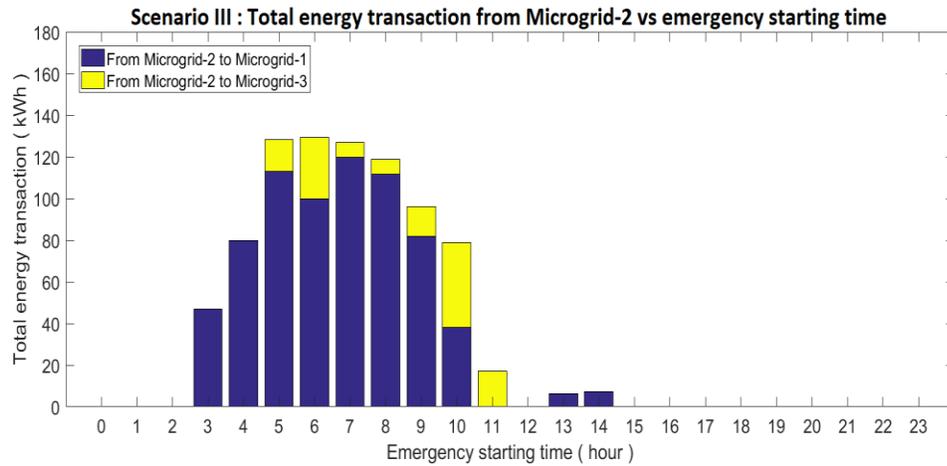
Figure 5.22 Scenario III: Total Energy Transaction from Microgrid-1 vs Emergency Starting Time
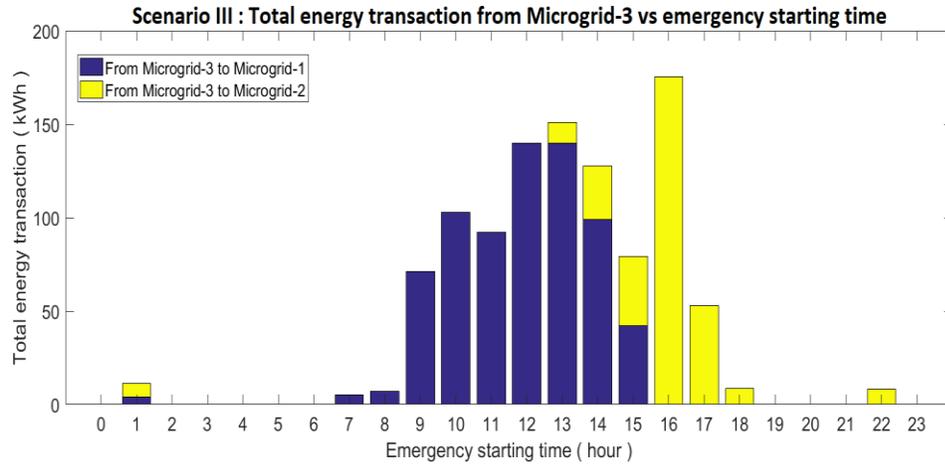
Figure 5.23 Scenario III: Total Energy Transaction from Microgrid-3 vs Emergency Starting Time

Due to the unavailability of the conventional DG installed in Microgrid-1, the total energy transaction from Microgrid-1 decreased compared to Scenario I. Additionally, the dependence of Microgrid-1 on energy transaction from Microgrid-2 and Microgrid-3 increased as deduced from the figures.

Even though the system was subjected to more severe emergencies, the proposed technique enhanced the overall performance and showed satisfactory performance. To prove this argument, the load restoration technique SI was calculated for emergencies with all possible starting times as shown in Figure 5.24. The maximum restoration success index was found to be 1.0697, while the mean was a satisfying 1.0546.
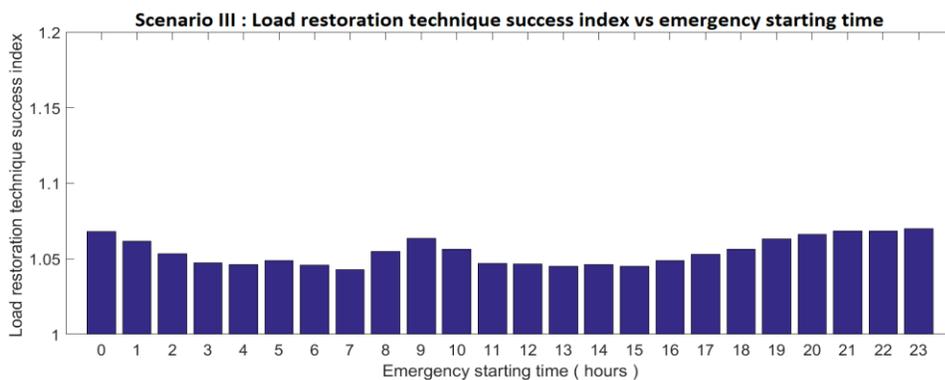
Figure 5.24 Scenario III: Load Restoration Technique Success Index vs Emergency Starting Time

83

5.3   Sensitivity Analyses

In this section, the impact of different parameters of the system on the performance of the load restoration technique is studied. Mainly, three sensitivity analyses were performed. Firstly, the impact of applying the preemptive load shifting DR program, and the percentage of allowable load shifting on the performance of the restoration technique was studied. Secondly, local optimization scheduling horizon was varied to examine its impact on the performance of the proposed restoration technique. Finally, a study was done to determine the sensitivity of the performance of the restoration technique to the capacity of the tie lines.

5.3.1 Sensitivity to Percentage of Shiftable Load

In this study, the percentage of shiftable loads at each time step varied. In other words, the maximum amount of allowable load shifting decided by the preemptive load shifting DR program varied. The value of the percentage varied in increments of 2.5% starting at 0% to 10%. Setting the value of the shiftable load percentage to 0% was done to simulate the case when DR was not applied. Scenario I was simulated for all different values of percentages and the average of the load restoration technique SI for emergencies with all possible starting times was calculated. This was done to study the impact of the DR program on the performance of the restoration technique. The resultant average success index for the deferent allowable load shifting percentages is summarized in Table 5.12.

Table 5.12 Sensitivity to Maximum Allowable Load Shifting Percentage

Sensitivity to Maximum Allowable Load Shifting Percentage					
Allowable percentage of load shifting	0%	2.5%	5%	7.5%	10%
Restoration technique success index	1.0517	1.0546	1.0567	1.0521	1.0486

As deduced from Table 5.12, the maximum allowable load shifting percentage should be selected carefully to ensure enhancement in the overall performance of the system. In general, applying the preemptive load shifting DR program enhanced the performance of the system, where the maximum load shifting percentage of 0% represents the case where the DR program is not applied. Allowing large amounts of load shifting may degrade the performance of the system as shown in the case of 10%. One explanation for this degradation can be that the large amount of load shifting can restrict the flexibility of the microgrids in supporting each other through energy transactions. For example, in Microgrid-2 allowing high percentage of load shifting will result in large amounts shifted to daytime hours where the generation is at its peak. As a consequence, most of the energy generated during these hours will be used to supply the local load, decreasing the ability of the Microgrid-2 to pick up disconnected loads in other microgrids.

5.3.2 Sensitivity to Local Scheduling Optimization Horizon

In the following study, Scenario I in which the MMG distribution system is subjected to an outage of 8 hours, is repeated for different values of the local optimization scheduling horizon. The summation of unsupplied energy for emergencies with all possible starting times is calculated for all different scheduling horizon values to study the impact of local scheduling horizon on the overall performance of the proposed restoration technique as shown in Table 5.13.

Table 5.13 Sensitivity to Local Scheduling Optimization Horizon

Sensitivity to Local Scheduling Optimization Horizon						
Scheduling Horizon (T_{Local})	2	3	4	6	8	10
Summation of total energy unsupplied [MWh]	3.9470	3.8740	4.0556	5.008	6.1482	6.5412

As evidenced in Table 5.13, choosing a smaller yet long enough, local scheduling optimization horizon yields better results in terms of the performance of the restoration technique. One justification for this is that microgrids that adopt long scheduling horizons may be more conservative and less willing to participate in the global scheduling. In addition, the effect of uncertainty in load demand and resource generation is more severe when longer optimization horizons are chosen.

5.3.3 Sensitivity to Tie Lines Capacity

The establishment of the capacity of tie lines is crucial to the performance of the restoration technique. The capacity of the tie lines should be determined according to the expected amount of energy transactions between microgrids. Tie lines with capacities much larger than the mean amount of energy transaction are not needed and add significant building costs to the system. On the other hand, installing small capacity tie lines can restrict the energy transactions between the microgrids, therefore reducing the performance of the restoration technique. In this study, Scenario I will be repeated for different values of tie lines capacity. The average load restoration technique SI for emergencies with all possible starting times will then be calculated to reflect the impact of the capacity of tie lines on the performance of the restoration technique as shown in (Table 5.14).

Table 5.14 Sensitivity to Tie Lines Capacity

Sensitivity to Tie Lines Capacity					
Capacity [kw]	8.75	17.5	35	50	75
Average success index	1.0253	1.0380	1.0543	1.0568	1.0568

As shown in Table 5.14, the capacity of tie lines impacts the performance of the restoration technique significantly. For example, there is an enhancement of about 25% on the performance when 50 kW tie lines are installed as opposed to the 8.75 kW tie lines. The performance is the same when 50 kW or 75 kW tie lines are installed. Thus, tie lines with a capacity of more than 50 kW are not needed and add unwanted expenses on the overall building cost of the system.

CHAPTER 6

CONCLUSION AND FUTURE WORK

In this chapter, the conclusion and the findings of the thesis are stated. The problem addressed, the solution proposed, and the resulting outcomes are indicated. Furthermore, the possibilities of extending this work on the future are also mentioned.

6.1   Conclusion

The main objective addressed in this work is to increase the resiliency of power systems against low-frequent high impact contingencies. In this context, a novel load restoration technique was proposed and tested. The performance of the proposed technique was reflected using novel formulated success index which take the performance of the power system before applying the restoration technique as a reference.

A comprehensive literature review was performed, defining, and visiting the relative work done in literature. In addition, the main underlying concepts and tools was defined and stated including the concept of smartgrids, microgrids and their control architectures, different types and strategies of EMSs, DMS and DR programs, and mathematical optimization. Afterward, the main components of microgrids was identified and introduced in addition to their mathematical modelling. Then, the proposed load restoration technique was formulated as MILP optimization problem in which a comprehensive mathematical formulation was built. Moreover, two DR programs were defined and incorporated to the

proposed load restoration technique namely, preemptively load shifting and emergency load shedding. Finally, a test system was build based on real life components and input data where real data of solar irradiance and ambient temperature, and residential load demand data measures in Dammam, Saudi was used as an instance.

The conclusions of the thesis can be summarized as:

- The proposed load restoration technique proved efficiency which was testified by performing comprehensive case studies.

- Sensitivity analysis was performed to study the impact of incorporating preemptive load shifting DR program. The DR program was found to enhance the overall performance of the system. However, large amount of load shifting caused a degradation on the performance of the proposed technique.

- It was proven that microgrids with shorter local scheduling optimization horizons participate more efficiently in the restoration process than those with longer horizons.

- The capacity of the tie lines was found to be very crucial to the performance of the proposed load restoration technique where suitable capacity must be chosen.

6.2   Future Work

In the future work, many aspects can be considered as a continuation of the work done in this thesis which include:

- The proposed restoration technique is formulated to be done for MMG distribution systems that is islanded from the main utility grid. Grid connected operation may be also be added to the formulation.

- The proposed load restoration technique is suitable for microgrids working in a cooperative-environment framework. Competitive operation environment can also be considered in the formulation of the restoration technique where benefits of applying the technique should be suitably distributed among the system agents.

- Power quality issues and transient condition of microgrids after the MMG distribution systems is islanded from the main utility grid may be addressed in the formulation of the restoration technique. This is mainly done by adding more constraints for the allowable deviations of microgrids voltages, currents and frequencies.

- The effectiveness of the restoration technique may also be verified by applying it on a real life microgrid test bed.

References

[1]   U.S. Department of Energy and National Energy Technology Laboratory, Operates Resiliently Against Attack and Natural Disaster [Online]. Available: http://www.smartgridinformation.info/pdf/1438_doc_1.pdf. [Accessed: December ,2016].

[2]   A.Khodaei,"Resiliency-Oriented Microgrid Optimal Scheduling," *IEEE Transactions on Smart Grid*, vol. 5, no. 4, pp. 1584-1591, 2014.

[3]   Electric Power Research Institute (EPRI), Tech. Rep., "Enhancing Distribution Resiliency – Opportunities for Applying Innovative Technologies", 2013

[4]   S.Ramchurn, P. Vytelingum, A. Rogers and N. Jennings, "Putting the "Smarts" into the Smart Grid: a grand challenge for artificial intelligence," *Commun. ACM*, pp. 86-96, 2012

[5]   A. Kenward and U. Raja, "Blackout: Extreme weather, climate change and power outages," Tech. Rep., Apr. 2014. [Online]. Available: http://www.ourenergypolicy.org/wp-content/uploads/2014/04/climate-central.pdf [Accessed: December ,2016].

[6]   Executive Office of the President, IEEE USA Books & eBooks, "Economic Benefits of Increasing Electric Grid Resilience to Weather Outages—USA", 2013 [online]:http://ieeexplore.ieee.org/xpl/articleDetails.jsp?arnumber=6978705. [Accessed: December ,2016].

[7]   "Climate change: Energy infrastructure risks and adaptation efforts,"U.S. Government Accountability Office, U.S. Dept. Energy, Jan. 2014, Washington, DC, USA.

[8]   CPLEX. IMM-ILOG, 2017. [online]: CPLEX.com

[9]   D. Abbott, "Keeping the Energy Debate Clean: How Do We Supply the World's Energy Needs?," *Proceedings of the IEEE*, vol. 98, no. 1, pp. 42-66, 2010.

[10]   F. Li et al., "Smart Transmission Grid: Vision and Framework," *IEEE Transactions on Smart Grid*, vol. 1, no.2, pp.168-177, 2010.

[11]   U.S. Department of Energy (DOE)'s, "Modern grid initiative," [online]: http://www.netl.doe.gov/moderngrid/ [Accessed: December ,2016].

[12]   S. Javadi, "Steps to smart grid realization," *Proceedings of WSEAS*, Cambridge, USA, pp. 223–228, 2010.

[13]   X. Yu and Y. Xue, "Smart grids: A cyber–physical systems perspective," *Proceedings of the IEEE*, vol. 104, no. 5, pp. 1058–1070, 2016.

[14]   M. sco r and D. Wg, "Impediments to the uptake of renewable and distributed energy:Discussion paper," p. 15, 2016.

[15]   B. Lasseter, "Microgrids [distributed power generation]," *2001 IEEE Power Engineering Society Winter Meeting. Conference Proceedings (Cat. No.01CH37194),* Columbus, OH, 2001, pp. 146-149.

[16]   H. Farzin, M. Fotuhi-Firuzabad and M. Moeini-Aghtaie, "Reliability Studies of Modern Distribution Systems Integrated with Renewable Generation and Parking Lots," *IEEE Transactions on Sustainable Energy*, vol. 8, no. 1, pp. 431-440, 2017.

[17]   T. Ustun, C. Ozansoy and A. Zayegh, "Recent developments in microgrids and example cases around the world. a review," *Renew. Sustain. Energy Rev.*, vol. 15, no. 8, pp. 4030-4041, 2011.

[18]   A. Maknouninejad, Z. Qu, F. L. Lewis and A. Davoudi, "Optimal nonlinear and distributed designs of droop controls for DC microgrids," *IEEE Trans. Smart Grid*, vol. 5, no. 5, pp. 2508-2516, 2014.

[19]   T. L. Vandoorn, J. C. Vasquez, J. De Kooning, J. M. Guerrero and L. Vandevelde, "Microgrids: Hierarchical Control and an Overview of the Control and Reserve Management Strategies," *IEEE Industrial Electronics Magazine*, vol. 7, no. 4, pp. 42-55, 2013.

[20]   Y. Riffonneau, S. Bacha, F. Barruel, and S. Ploix, "Optimal power flow management for grid connected PV systems with batteries," *IEEE Trans. Sustain. Energy*, vol. 2, no. 3, pp. 309–320, 2011.

[21]   H. Ren and W. Gao, "A MILP model for integrated plan and evaluationof distributed energy systems," *Appl. Energy*, vol. 87, no. 3, pp. 1001–1014, 2010

[22]   C. Chen, S. Duan, B. Liu, and G. Hu, "Smart energy management system for optimal microgrid economic operation," *IET Renew. Power Generat.*, vol. 5, no. 3, pp. 258–267, 2011.

[23]   M. Elsied, A. Oukaour, H. Gualous, R. Hassan and A. Amin, "An advanced energy management of microgrid system based on genetic algorithm," *2014 IEEE 23rd International Symposium on Industrial Electronics (ISIE)*, Istanbul, Turkey, 2014, pp. 2541-2547.

[24] N. Nikmehr and S. N. Ravadanegh, "Optimal power dispatch of multimicrogrids at future smart distribution grids, " *IEEE Trans. Smart Grid*, vol.6, no. 4, pp. 1648–1657, 2015.

[25] D. E. Olivares, C. A. Cañizares, and M. Kazerani, "A centralized energy management system for isolated microgrids, " *IEEE Trans. Smart Grid*, vol. 5, no. 4, pp. 1864–1875, 2014.

[26] Z. Wang, B. Chen, and J. Kim, "Decentralized energy management system for networked microgrids in grid-connected and islanded modes, " *IEEE Trans. Smart Grid*, vol. 7, no. 2, pp. 1097–1105, 2016.

[27] P. Tian, X. Xiao, K. Wang and R. Ding, "A Hierarchical Energy Management System Based on Hierarchical Optimization for Microgrid Community Economic Operation," *IEEE Transactions on Smart Grid*, vol. 7, no. 5, pp. 2230-2241, 2016.

[28] V. H. Bui, A. Hussain and H. M. Kim, "A Multiagent-Based Hierarchical Energy Management Strategy for Multi-Microgrids Considering Adjustable Power and Demand Response," *IEEE Transactions on Smart Grid*, vol. PP, no. 99, pp. 1-1, 2016. doi: 10.1109/TSG.2016.2585671

[29] K. P. Schneider, F. K. Tuffner, M. A. Elizondo, C. C. Liu, Y. Xu and D. Ton, "Evaluating the Feasibility to Use Microgrids as a Resiliency Resource," *IEEE Transactions on Smart Grid*, vol. 8, no. 2, pp. 687-696, March 2017.

[30] H. Jia, X. Jin, Y. Mu and X. Yu, "A multi-level service restoration strategy of distribution network considering microgrids and electric vehicles," 2014 *International Conference on Intelligent Green Building and Smart Grid (IGBSG)*, Taipei, pp. 1-4, 2014

[31] Y. Xu, C. C. Liu, K. Schneider, F. Tuffner and D. Ton, "Microgrids for Service Restoration to Critical Load in a Resilient Distribution System," *IEEE Transactions on Smart Grid*, vol. PP, no. 99, pp. 1-1, 2016.

[32] C. Gouveia, J. Moreira, C. L. Moreira, and J. A. Pecas Lopes, "Coordinating storage and demand response for microgrid emergency operation," *IEEE Trans. Smart Grid*, vol. 4, no. 4, pp. 1898–1908, 2013.

[33] S. Bessler, D. Hovie and O. Jung, "Outage response in microgrids using demand side management," *2016 IEEE International Smart Cities Conference (ISC2)*, Trento, Italy, 2016, pp. 1-6.

[34] K. Balasubramaniam, P. Saraf, R. Hadidi, and E. B. Makram, "Energy management system for enhanced resiliency of microgrids during islanded operation," *Electric Power Systems Research,* vol. 137, pp. 133 – 141, 2016.

[35] S. A. Pourmousavi, M. H. Nehrir and R. K. Sharma, "Multi-Timescale Power Management for Islanded Microgrids Including Storage and Demand Response," *IEEE Transactions on Smart Grid*, vol. 6, no. 3, pp. 1185-1195, 2015.

[36] C. Gouveia, C. L. Moreira, J. A. P. Lopes, D. Varajao and R. E. Araujo, Microgrid Service Restoration: The Role of Plugged-in Electric Vehicles," *IEEE Industrial Electronics Magazine*, vol. 7, no. 4, pp. 26-41, 2013.

[37] H. Farzin, M. Fotuhi-Firuzabad and M. Moeini-Aghtaie, "Reliability Studies of Modern Distribution Systems Integrated with Renewable Generation and Parking Lots," *IEEE Transactions on Sustainable Energy*, vol. 8, no. 1, pp. 431-440, 2017.

[38] S. M. Mohammadi-Hosseininejad, A. Fereidunian, A. Shahsavari and H. Lesani, "A Healer Reinforcement Approach to Self-Healing in Smart Grid by PHEVs Parking Lot Allocation," *IEEE Transactions on Industrial Informatics*, vol. 12, no. 6, pp. 2020-2030, 2016.

[39] "IEEE Guide for Design, Operation, and Integration of Distributed Resource Island Systems with Electric Power Systems, "*IEEE Standard 1547.4-2011*, pp. 1-54, 2011.

[40] M. Goyal and A. Ghosh, "Microgrids interconnection to support mutually during any contingency", *Sustainable Energy Grids and Networks*, vol. 6, pp. 100-108, 2016.

[41] Z. Wang, B. Chen, J. Wang and C. Chen, "Networked Microgrids for Self-Healing Power Systems,"*IEEE Trans. Smart Grid*, 2016.

[42] A. Hussain, V. H. Bui and H. M. Kim, "A Resilient and Privacy-Preserving Energy Management Strategy for Networked Microgrids," *IEEE Transactions on Smart Grid*, vol. PP, no. 99, pp. 1-1, 2017.

[43] C. Chen, J. Wang, F. Qiu and D. Zhao, "Resilient Distribution System by Microgrids Formation After Natural Disasters," *IEEE Transactions on Smart Grid*, vol. 7, no. 2, pp. 958-966, 2016.

[44]   J. S. Vardakas, N. Zorba and C. V. Verikoukis, "A Survey on Demand Response Programs in Smart Grids: Pricing Methods and Optimization Algorithms," *IEEE Communications Surveys & Tutorials*, vol. 17, no. 1, pp. 152-178, Firstquarter 2015.

[45]   P. Palensky and D. Dietrich, "Demand Side Management: Demand Response, Intelligent Energy Systems, and Smart Loads," *IEEE Transactions on Industrial Informatics*, vol. 7, no. 3, pp. 381-388, 2011.

[46]   R. Deng, Z. Yang, M. Y. Chow and J. Chen, "A Survey on Demand Response in Smart Grids: Mathematical Models and Approaches," *IEEE Transactions on Industrial Informatics*, vol. 11, no. 3, pp. 570-582, 2015.

[47]   H. T. Haider, O. H. See, and W. Elmenreich, "A review of residential demand response of smart grid," *Renew. Sustain. Energy Rev.,* vol. 59, pp. 166–178, 2016

[48]   N. Ruiz, I. Cobelo, and J. Oyarzabal, "A direct load control model for virtual power plant management," *IEEE Trans. Power Syst.*, vol. 24, no. 2, pp. 959–966, 2009.

[49]   H. A. Aalami, M. P. Moghaddam, and G. R. Yousefi, "Demand response modeling considering Interruptible/Curtailable loads and capacity market programs," *Appl. Energy*, vol. 87, no. 1, pp. 243–250, 2010.

[50]   Y. Wang, I. R. Pordanjani, and W. Xu, "An event-driven demand response scheme for power system security enhancement," *IEEE Trans. Smart Grid*, vol. 2, no. 1, pp. 23–29, 2011.

[51]   H. S. Oh and R. J. Thomas, "Demand-side bidding agents: Modeling and simulation," *IEEE Trans. Power Syst*., vol. 24, no. 3, pp. 1050–1056, 2008.

[52]   S. Zhao and Z. Ming, "Modeling demand response under time-of-use pricing," *2014 International Conference on Power System Technology*, Chengdu, 2014, pp. 1948-1955.

[53]   X. Zhang, "Optimal Scheduling of Critical Peak Pricing Considering Wind Commitment," *IEEE Transactions on Sustainable Energy*, vol. 5, no. 2, pp. 637-645, 2014.

[54]   L. Gomes, F. Fernandes, P. Faria, M. Silva, Z. Vale and C. Ramos, "Real-time simulation of real-time pricing demand response to meet wind variations," *IEEE PES Innovative Smart Grid Technologies*, Europe, Istanbul, 2014, pp. 1-6.

[55]   F. Katiraei, R. Iravani, N. Hatziargyriou, and A. Dimeas, "Microgrids management, " *IEEE Power and Energy Magazine*, vol. 6, no. 3, pp. 54–65, 2008.

[56]   "International energy outlook 2013*"US Energy Information Administration (EIA)*, Report Number: DOE/EIA-0484, 2017.

[57]   J. Sawin "Renewable energy policy network for the 21st century: Renewables 2011 Global Status Report, technical report" REN21 Secretariat, Paris, 2011

[58]   "Snapshot of Global Photovoltaic Markets 2017," *International Energy Agency (IEA)*, Report Number: IEA PVPS T1-31, 2017.

[59]   W. Palz, Power for the World: The emergence of electricity from the sun, Panstanford Publishing, 2010.

[60]   M. G. Villalva, J. R. Gazoli and E. R. Filho, "Comprehensive Approach to Modeling and Simulation of Photovoltaic Arrays," *IEEE Transactions on Power Electronics*, vol. 24, no. 5, pp. 1198-1208, 2009.

[61]   J. Nelson, The Physics of Solar Cells, U.K., London:Imperial College Press, 2003.

[62]   NASA Science Beta (2012). [image] Available at: https://science.nasa.gov/science-news/science-at-nasa/2002/solarcells [Accessed: December ,2016].

[63]   A. Goetzberger, V. U. Hoffmann, Photovoltaic Solar Energy Generation, Germany, Berlin:Springer-Verlag, 2005.

[64]   Electrical Technology (2015). Basic operating principle of solar cells. [image] Available at: https://www.electricaltechnology.org/2015/06/, [Accessed: December 2016].

[65]   Hyeonah Park and Hyosung Kim, "PV cell modeling on single-diode equivalent circuit," *IECON 2013 - 39th Annual Conference of the IEEE Industrial Electronics Society*, Vienna, Austria, 2013, pp. 1845-1849.

[66]   V. Tamrakar, S. C. Gupta and Y. Sawle, "Study of characteristics of single and double diode electrical equivalent circuit models of solar PV module," *2015 International Conference on Energy Systems and Applications*, Pune, India, 2015, pp. 312-317.

[67]   B. Jacob, K. Balasubramanian and T. S. Babu and N. Rajasekar, "Parameter extraction of solar PV double diode model using artificial immune system," *2015 IEEE International Conference on Signal Processing, Informatics, Communication and Energy Systems (SPICES)*, Kozhikode, India, 2015, p. 1-5.

[68]   H. Bellia, R. Youcef and M. Fatima,"A Detailed Modeling of Photovoltaic Module Using MATLAB,"*NRIAG Journal of Astronomy and Geophysics*, vol. 3, pp. 53-61, 2014

[69]   N. Mohammad, M. Quamruzzaman, M. Hossain and M. Alam "Parasitic Effects on The Performance of Dc/Dc Sepic in Photovoltaic Maximum Power Point Tracking Applications " *Smart Grid and Renewable Energy: scientific research,* vol. 4, no. 1, pp. 113-121, 2013.

[70]   D.R. Myers, "Evaluation of the Performance of the PVUSA Rating Methodology Applied to Triple Junction PV Technology", *American Solar Energy Society Annual Conference 2009*, Buffalo, New York, 2009.

[71]   C. M. Whitaker, T. U. Townsend, H. J. Wenger, A. Iliceto, G. Chimento and F. Paletta, "Effects of irradiance and other factors on PV temperature coefficients," *The Conference Record of the Twenty-Second IEEE Photovoltaic Specialists Conference - 1991*, Las Vegas, NV, 1991, pp. 608-613 vol.1.

[72]   B. Marion, B. Kroposki, K. Emery, J. del Cueto, D. Myers, and C. Osterwald, "Validation of a photovoltaic module energy ratings procedure at NREL," *NREL* Technical Report, 1999.

[73]   D. K. Khatod, V. Pant, and J. Sharma, "Analytical approach for wellbeing assessment of small autonomous power systems with solar and wind energy sources," *IEEE Trans. Energy Convers.*, vol. 25, no. 2, pp. 535–545, 2010.

[74]   "Renewable capacity highlights 2017, " *International Renewable Energy Agency (IRENA)*,2017.   ISBN :978-92-9260-018-1.

[75]   G. M. Masters, Renewable and Efficient Electric Power Systems. Wiley, 2004.

[76]   S. Diaf, D. Diaf, M. Belhamel, M. Haddadi, and A. Louche, "A methodology for optimal sizing of autonomous hybrid PV/wind system," *Energy Policy*, vol. 35, pp. 5708–5718, 2007.

[77]   Q. Lin and J. Wang, "Vertically Correlated Echelon Model for the Interpolation of Missing Wind Speed Data," *IEEE Transactions on Sustainable Energy*, vol. 5, no. 3, pp. 804-812, 2014.

[78]   S. Ramabhotla, S. Bayne and M. Giesselmann, "Economic dispatch optimization of microgrid in islanded mode," *International Energy and Sustainability Conference 2014*, Farmingdale, NY, 2014, pp. 1-5.

[79]   A. K. Daud and M. S. Ismail, "Design of isolated hybrid systems minimizing costs and pollutant emissions", *Renew. Energy*, vol. 44, pp. 215-224, 2012.

[80]   A. Joseph and M. Shahidehpour, "Battery storage systems in electric power systems," *2006 IEEE Power Engineering Society General Meeting,* Montreal, Que., Canada, 2006, pp. 1-8.

[81] S. Bahramirad and W. Reder, "Islanding applications of energy storage system," *2012 IEEE Power and Energy Society General Meeting*, San Diego, CA, 2012, pp. 1-5. doi: 10.1109/PESGM.2012.6345706

[82] B. E. Layton, "A comparison of Energy Densities of Prevalent Energy Sources in Units of Joules Per Cubic Meter," *International Journal of Green Energy*, vol. 5, no. 6, pp. 438-455, 2008.

[83] Y. Yoldas, A. Onen, S. Muyeen, A. V. Vasilakos, and I. Alan, "Enhancing smart grid with microgrids: Challenges and opportunities, *" Renewable and Sustainable Energy Reviews,* vol. 72, pp. 205-214, 2017.

[84]   H. Bergveld, *Battery management systems design by modelling*, Univ. Twente, 2001.

[85] J. A. Jardini, C. M. V. Tahan, M. R. Gouvea, S. U. Ahn, and F.M. Figueiredo, "Daily load profiles for residential, commercial and industrial low voltage consumers," *IEEE Trans. Power Del.,* vol. 15, no. 1, pp. 375–380, 2000.

[86] Jun-Hyeok Son and Bo-Hyeok Scriber, "Problem solution of linear programming using dual simplex method neural network," *2005 International Conference on Electrical Machines and Systems*, Nanjing, Chaina, 2005, pp. 2045-2047, vol. 3.

[87] Y. Mezentsev, "Binary cut-and-branch method for solving mixed integer programming problems," *2017 Constructive Nonsmooth Analysis and Related Topics (dedicated to the memory of V.F. Demyanov) (CNSA),* St. Petersburg, 2017, pp. 1-3.

[88] P.Venkataraman, Applied Optimization with MATLAB Programming.Wiley, 2009.

[89] MITSUBISHI ELECTRIC, "MLU series Photovoltaic Modules," PV-MLU255HC, datasheet.

[90] S. Rehman, T. Halawani, and T. Husain, "Weibull parameters for wind speed distribution in Saudi Arabia," *Solar Energy*, vol. 53, no. 6, pp. 473–479, 1994.

[91] S. Sarkar and V. Ajjarapu, "MW Resource Assessment Model for a Hybrid Energy Conversion System with Wind and Solar Resources," *IEEE Transactions on Sustainable Energy*, vol. 2, no. 4, pp. 383-391, 2011.

[92] raum Energy, "3.5 kW wind turbine system," datasheet.

Vitae

Name   : Moheeb Ott

Nationality   : Jordanian

Date of Birth   : 31/3/1992

 Email   : Moheeb-k@outlook.com

Address   : 2567 Dareen ST, Rabwa Dist.
                                          RIYADH 12834-7307
                                          SAUDI ARABIA

Academic Background:

2018: **MS** in Electrical Engineering

       KING FAHD UNIVERSITY OF PETROLEUM AND MINERALS, Saudi Arabia

2015: **BS** in Electrical Engineering

       KING FAHD UNIVERSITY OF PETROLEUM AND MINERALS, Saudi Arabia

2010: **high secondary school certificate**

       Al Faisaliah secondary school, Riyadh, Saudi Arabia